UPPSALA
UNIVERSITET

Digital Comprehensive Summaries of Uppsala Dissertations from the Faculty of Science and Technology 2170

Development of phosphorus-containing metallo-β-lactamase inhibitors

Synthesis and binding studies by solution NMR and molecular docking

KATARZYNA PALICA

ACTA
UNIVERSITATIS
UPSALIENSIS
UPPSALA
2022

ISSN 1651-6214
ISBN 978-91-513-1561-4
URN urn:nbn:se:uu:diva-481327

Dissertation presented at Uppsala University to be publicly examined in A1:111a, Husargatan 3, Uppsala, Monday, 26 September 2022 at 09:15 for the degree of Doctor of Philosophy. The examination will be conducted in English. Faculty examiner: Professor Christopher J. Schofield (University of Oxford).

Abstract

Palica, K. 2022. Development of phosphorus-containing metallo-β-lactamase inhibitors. *Synthesis and binding studies by solution NMR and molecular docking . Digital Comprehensive Summaries of Uppsala Dissertations from the Faculty of Science and Technology* 2170. 67 pp. Uppsala: Acta Universitatis Upsaliensis. ISBN 978-91-513-1561-4.

The rapidly growing bacterial resistance development is turning into one of the main challenges of the 21st century. Our antibiotics are becoming ineffective for the treatment of bacterial infections, and without successful action, simple infections, such as pneumonia or Septicemia, will soon carry a highly probable mortal prognosis. Among the most widely spread mechanisms of bacterial resistance are the degradation and modification of antibiotics, prior to them reaching the target site, by bacterial enzymes.

This thesis work aims to contribute to solving a major societal challenge by providing new knowledge on the binding site of the NDM-1, which is one of the clinically most relevant enzymes used by bacteria to degrade antibiotics. The work includes the design and synthesis of potential β-lactamase inhibitors that mimic the transition state of the enzymatic hydrolysis of β-lactam antibiotics. These bioisosteric transition state analogues are expected to bind and inhibit NDM-1, without being hydrolysable. Thereby they could potentially slow down or even halt the degradation of our β-lactam antibiotics is use.

The first chapter describes the specific aims, whereas the second presents a general overview of bacterial resistance showing the mechanism of β-lactam hydrolysis along with our current knowledge of the structure of metallo-β-lactamases and examples for known inhibitors. The third chapter reviews the key features of the applied methods including those of enzyme assays, NMR protein backbone resonance assignment, chemical shift perturbation, NOESY and molecular docking. Subsequently, the investigation of the three groups of metallo-β-lactamase inhibitors are discussed. First, the design and synthesis of phosphoamidate- and phosphonic acid-based metallo-β-lactamase inhibitors is presented. Subsequently, enzyme - inhibitor binding studies as well as combined solution NMR spectroscopic and computational docking studies aiming the determination of binding site and pose of inhibitor candidates is described. The binding affinities and binding modes for three types of enzyme inhibitors are disclosed along with a comparison of their binding to the New Delhi metallo-β-lactamase (NDM-1) and Verona integron-encoded metallo-β-lactamase (VIM-2), pointing out similarities and differences. The binding pose of a previously developed inhibitor has also been determined with the help of fluorine-labeling.

The knowledge generated in this thesis work is expected to be useful for the development of wide spectrum metallo-β-lactamase inhibitors, which may become a long-sought relief in an escalating crisis.

Keywords: MBL inhibitors; antibiotic resistance; metallo-β-lactamases, NMR spectroscopy

Katarzyna Palica, Department of Chemistry - BMC, Organic Chemistry, Box 576, Uppsala University, SE-75123 Uppsala, Sweden.

ISSN 1651-6214
ISBN 978-91-513-1561-4
URN urn:nbn:se:uu:diva-481327 (http://urn.kb.se/resolve?urn=urn:nbn:se:uu:diva-481327)

“That’s what you seek. You want to find something that looks absurd and figure out how to do it."
Tommy Caldwell

List of Papers

This thesis is based on the following papers, which are referred to in the text by their Roman numerals.

I. Palica, K.; Vorácová, M.; Skagseth, S.; Andersson Rasmussen, A.; Allander, L.; Hubert, M.; Sandegren, L.; Schrøder Leiros, H. K.; Andersson, H. ; Erdelyi, M. (2022) Metallo-β-Lactamase Inhibitor Phosphonamidate Monoesters. *ACS Omega*, 7:4550–4562.

II. Palica, K.; Deufel, F.; Skagseth, S.; Andersson Rasmussen, A.; Schroder Leiros, H. K.; Sunnerhagen, P.; Andersson, H.; Erdélyi, M., Phosphonate inhibitors of metallo-β-lactamases NDM-1 and VIM-2, *Submitted.*

III. Palica, K.; Kondratieva A., Skagseth, S.; Schroder Leiros, H. K.; Bayer A.; Erdelyi M., The binding site and binding mode of a simplified captopril analogue, established via fluorine labelling, *Manuscript*

Other documents this thesis is based on

The content of this thesis is partially built upon the author's half-time report presented on September 11th, 2020. Chapters 2, 3.1, 4.2, and 6.2 have been based on the half-time report; the rest of the thesis was written from the scratch.

Contents

1. Aim of the thesis 11

2. Introduction 12
   2.1. Bacterial resistance 12
   2.2. The hydrolysis mechanisms of β-lactamases 14
   2.3. The structure of metallo-β-lactamases 16
   2.4. Known metallo-β-lactamases inhibitors 17

3. Overview of methods 23
   3.1. Enzyme assay 23
   3.2. Protein backbone assignment 24
   3.3. Chemical shift perturbation 28
   3.4. NOESY based experiments 30
   3.5. Molecular docking studies 31

4. New metallo-β-lactamase inhibitors 33
   4.1. Phosponamidate-based MBL inhibitors (Paper I) 34
   4.2. Phosphonic acid-based MBL inhibitors (Paper II) 37
   4.3. Fluorine-labelled MBL inhibitors (Paper III) 38

5. Metallo-β-lactamase binding 39
   5.1. Metallo-β-lactamase inhibitory activity 39
   5.2. Protein-ligand interactions - studied by NMR 41
   5.3. NMR spectroscopic determination of the binding site of the inhibitors 43
   5.4. Molecular docking studies 50

6. Concluding remarks and perspective 55

7. Sammanfattning på Svenska 57

8. Acknowledgements 59

9. References 62

Abbreviations

AA	Amino acid
ASL	Active site loop
BL	β-lactamase
cLogP	Partition coefficient using group contributions
COMU	(1-Cyano-2-ethoxy-2-oxoethylidenaminooxy)dimethyl-amino-morpholino-carbenium hexafluorophosphate
CSP	Chemical shift perturbation
DCM	Dichloromethane
DEAD	Diethyl azodicarboxylate
DMSO	Dimethyl sulfoxide
DME	1,2-Dimethoxyethane
eq	Equivalent
EWG	Electron withdrawing group
GIM	German imipenemase metallo-β-lactamase
HATU	1-[Bis(dimethylamino)methylene]-1H-1,2,3-triazolo[4,5-*b*]pyridinium 3-oxid hexafluorophosphate
HOBt	1-Hydroxybenzotriazole hydrate
HOE	Heteronuclear Overhauser Effect
HOESY	Heteronuclear Overhauser Effect Spectroscopy
HPLC	High-performance liquid chromatography
HSQC	Heteronuclear single quantum coherence spectroscopy
IC_{50}	Half maximal inhibitory concentration
K_d	Equilibrium dissociation constant
$LiBH_4$	Lithium borohydride
LiBr	Lithium bromide
MBL	Metallo-β-lactamase
MBLI	Metallo-β-lactamase inhibitor
MM-GBSA	Molecular mechanics with generalized Born and surface area solvation
NaH	Sodium hydride
NaI	Sodium iodide
NDM	New Delhi metallo-β-lactamase
NMR	Nuclear magnetic resonance
NOESY	Nuclear Overhauser effect spectroscopy
NUS	Non-uniform sampling

$O=PPh_3$	Triphenylphosphine oxide
Oxyma	Ethyl cyanohydroxyiminoacetate
PBP	Penicillin-binding proteins
PDB	Protein Data Bank
PPh_3Cl_2	Triphenylphosphine dichloride
$PS\text{-}PPh_3$	Triphenylphosphine, polymer-bound
PyAOP	(3-Hydroxy-3H-1,2,3-triazolo[4,5-b]pyridinato-O)tri-1-pyrrolidinyl-phosphorus hexafluorophosphate
PyBOP	(Benzotriazol-1-yloxy)tripyrrolidinophosphonium hexafluorophosphate
r.t.	Room temperature
SAR	Structure-activity relationship
SBL	Serine-β-lactamase
SSP	Significant shift perturbation
TCEP	Tris(2-carboxyethyl)phosphine
THF	Tetrahydrofuran
VIM	Verona integron-encoded metallo-β-lactamase
WHO	World health organization
δ	Chemical shift
μ+σ	The population mean plus standard deviation

<u>20 naturally occurring amino acids</u>

Amino acid full name	Three letter	One letter
Alanine	Ala	A
Arginine	Arg	R
Asparagine	Asn	N
Aspartic Acid	Asp	D
Cysteine	Cys	C
Glutamic acid	Glu	E
Glutamine	Gln	Q
Glycine	Gly	G
Histidine	His	H
Isoleucine	Iso	I
Leucine	Leu	L
Lysine	Lys	K
Methionine	Met	M
Phenylalanine	Phe	F
Proline	Pro	P
Serine	Ser	S
Threonine	Thr	T
Tryptophan	Trp	W
Tyrosine	Tyr	Y
Valine	Val	V

1. Aim of the thesis

The overall goal of this thesis work is the development of new metallo-β-lactamase inhibitors, and the structural investigation of their complexes with the target enzymes. These aims provide the basis for a future development of clinically available inhibitors.

The specific objectives are to:

- design and synthesize a series of potential inhibitors,
- provide NMR assignment for the backbone of NDM-1,
- determine the active site of the enzyme using solution NMR,
- visualize the binding site and mode with computational docking.

2. Introduction

2.1. Bacterial resistance

Alexander Fleming's discovery of penicillin (1929)[1] was a grand achievement of the 20th century. Shortly after its discovery, penicillin became the first commercially available and the most used antibiotic.[2] World War II dramatically increased its consumption. The lack of alternatives for treating bacterial infections induced the development of penicillin-resistant strains. Accordingly, already in the 1940s, 59% of the patients were infected by penicillin-resistant bacteria.[3] The high demand for treatment of bacterial infections, the rapid development of new antibiotics between the 1940s and the 1980s,[4] and a continuous overuse of antibiotics led to one of mankind's crises, according to the World Health Organization (WHO).[5]

Our current antibiotics can be divided into various classes.[6] Within a specific class a high degree of structural similarity exists, which leads to the unavoidable disadvantage that bacteria gaining resistance to one specific drug typically becomes insensitive also to the entire antibiotic class the drug belongs to. Additionally, unproblematic transmission of genes, such as the bla_{NDM}, was observed among different types of gram-negative organisms.[7] In other words, bacteria can transfer resistance from one strain to another and thereby spread it.

Microbial infections became one of the main challenges of the XXI century. Published in 2014, the WHO global report on surveillance of antimicrobial resistance pointed out the high prevalence of community-acquired infections that are caused by antibiotic-resistant bacteria.[8] The problematic bacteria commonly triggering infections include *Enterobacteriaceae*, *Escherichia coli*, *Klebsiella pneumonia*, and *Acinetobacter baumanniiare*. These were reported to be resistant to the 3rd generation cephalosporins and even to carbapenems, which are often called the antibiotics of last resort.[8] The number of deaths caused by antibiotics resistant bacteria is estimated to reach 10 million per year by 2050, according to an Independent Review on AMR (antimicrobial resistance), chaired by Lord O'Neill.[9] This reflects the enormous need for alternative treatments for bacterial infections.[10-11]

We are in an antibiotic discovery void since the 1980s, when the number of newly developed antibiotic classes dramatically dropped.[12] Thereto, β-lactam antibiotics efficacy against microbes is declining due to rapid resistance development that was promoted by a wide misuse of antibiotics. The main mechanisms for bacterial resistance[13-17] are (*i*) the production of β-lactam-hydrolyzing β-lactamase enzymes, (*ii)* target alteration by modification of the antibiotics target - penicillin-binding proteins (PBPs), (*iii*) the active expulsion of β-lactams from cells by efflux pumps, and (*iv*) reduced membrane permeability. The upcoming crisis is apparent, and therefore multiple strategies are being developed to combat antibiotic resistant bacteria.

Whereas the natural occurrence of antimicrobial resistance cannot be avoided, human actions that aggravate the development and spread of resistance can be restricted. This may include the enforcement of a limited usage of antibiotics for the treatment of both human and animal diseases.[18]However, the worldwide implementation of such a restriction is not straightforward. For instance, antibiotics are often used as growth support and for the prevention of animal infections, rather than for disease treatment. In addition, in countries with poor clinical practices antibiotics are prescribed also for the treatment of viral infections.[19]

The low profit and the high-risk of investing in developing new treatments for resistant bacterial infections turned academic research to the driving force of new developments.[20] A promising concept to fight resistance against β-lactam antibiotics is the use of combination therapy, which includes the use of MBL/SBL inhibitors together with existing antibiotics.[21] Several studies proved this approach to be efficient and noted lower resistance levels as compared to that observed with traditional antibiotic treatments.[22-24] Commercially available and clinically applicable serine-β-lactam inhibitors exist, whereas so far no metallo-β-lactamase inhibitors have yet reached the market, and so far only two are in clinical trials.[25] Even though there seems to be a straightforward pathway to follow for developing such inhibitors, the structural variation of metallo-β-lactamases narrow the spectrum and the usefulness of inhibitors. So far β-lactam analogues give the best inhibition of β-lactamases. For fruitful inhibitor design, a good understanding of the mechanism of enzyme action, which leads to the degradation of β-lactam antibiotics, is necessary. Based on mechanistic studies and on the structure of existing inhibitors, plenty of possible inhibitors were proposed.[26] This project focuses on the development of analogues of the tetrahedral transition state of the enzymatic β-lactam hydrolysis process, also making use of the knowledge gained from existing antibiotics and from structural NMR spectroscopic[27-28] and computational investigations. Upon succeeding, this work is expected to provide knowledge useful for the rational design of new inhibitors of β-lactamases and thereby elimination of one of the most distressing routes of antibiotic resistance.

Fleming's prediction (1945, Nobel lecture) on the development of bacterial resistance as a consequence of antibiotics overuse has become reality.[29] Most of the bacterial resistance is connected to the microbial cell wall, which contains a cross-linked peptidoglycan layer for both Gram-positive and Gram-negative bacteria. The layer is constructed from repeating units of the disaccharides *N*-acetyl glucosamine and *N*-acetyl muramic acid, and is terminated with two *D*-alanine residues.[30] This cell wall is responsible for the shape and the integrity of the bacteria, upon exposure to osmotic pressure, for example. With a structure mimicking the *D*-Ala-*D*-Ala terminus, the targets of β-lactam antibiotics are penicillin binding proteins, PBPs (Figure 1). A grand contribution to Gram-negative resistance originates from bacterial β-lactamases, which hydrolyze and thereby inactivate β-lactam antibiotics.

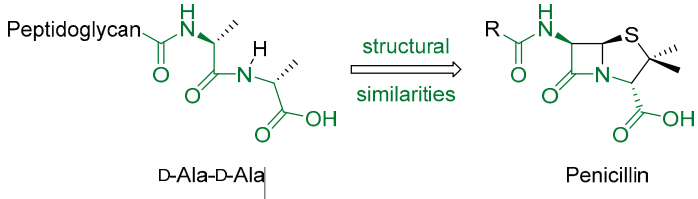

Figure 1. Penicillin-type antibiotics resemble the structure of the *D*-Ala-*D*-Ala terminus of the peptidoglycans of the bacterial cell wall.

2.2. The hydrolysis mechanisms of β-lactamases

β-Lactamases are categorized according to the Ambler classification. Ambleroriginally divided those enzymes according to their amino acid sequence, and the classification primarily was represented by groups A, and B.[31] Discovery of protein with lower degree of connection to group A (AmpC β-lactamases)[32] and another sequence alteration of A and C (OXA β-lactamases)[33] resulted in establishing four groups; A, B, C and D. Later, Hall and Barlow[34] revised classification and implemented division of the β-lactamases to main groups: metallo-β-lactamases (MBLs) and serine-β-lactamases (SBLs) according their antibiotics hydrolysis mechanism. Metallo-β-lactamases are additionally divided, to B1, B2, and B3 subclasses,[34] based on the structural homology and they require one or two zinc ions in their active center.[35] In the case of serine-β-lactamases, the hydroxyl group of a serine, as the name indicates, acts as the nucleophile and initiates the hydrolysis, utilizing an acylation/deacylation mechanism.[36] The common step of these mechanisms is tocreate a highly energetic tetrahedral intermediate. This step leads to irreversible changes in the structure of the β-lactam antibiotics since the C-N bond of the β-lactam ring gets cleaved.

Belonging to the A, C, and D classes are serine-β-lactamases. One of the reported mechanisms for class A is presented below, using general peneme-type antibiotics as an example. (Figure 2) The first step is considered to occur through acylation create the acyl-enzyme complex (Henri-Michaelis, the high energy tetrahedral intermediate ‡EI^1) by nucleophilic attack of the active site Ser70-hydroxy group. The lower energy of the hydrolyzed product is the result of the cleavage of the high-energy four-member β-lactam ring. Subsequently, the amine is protonated, and a covalent bond is formed between the antibiotic and the enzyme, yielding an acyl-enzyme complex. In the following steps, the nucleophilic attack of water generates a high-energy intermediate (tetrahedral intermediate ‡EI^2), from which Ser70 is eliminated. An inactive version of the antibiotic is released, and then the enzyme is regenerated.

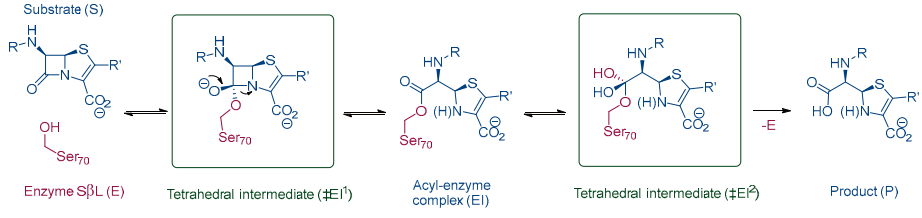

Figure 2. The mechanism of hydrolysis of penem-type antibiotics by serine- β-lactamases.[37]

The group of enzymes in the interest of this thesis are classified as Class B β-lactamase – metallo-β-lactamases. They have a different structure and act mechanistically different as compared to SBLs (Figure 3). The mechanism of their action starts with the coordination of one or two zinc ions to the oxygen of the β-lactam's carboxylic group and to the oxygen of the β-lactam ring. The zinc ions of the active site are essential for the activity of these enzymes, although the specific role of the two ions remains a matter of debate. The proposed nucleophile is a hydroxide ion, which bridges the zinc ions. The nucleophilic attack of the hydroxide on the carbonyl carbon leads to a tetrahedral intermediate (‡EI). This step, similar to the mechanism of serine-β-lactamases, is followed by irreversible changes. Next, an anionic intermediate is formed as a result of the C-N bond cleavage of the β-lactam ring. Finally, protonation yields enzyme cleavage and an inactive form of the antibiotic.[38]

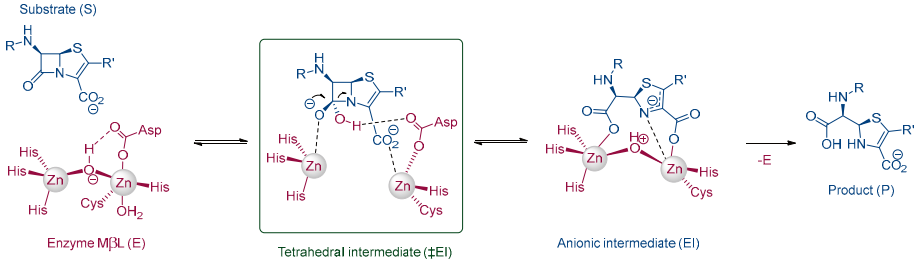

Figure 3. Mechanism of hydrolysis of penem-type antibiotics by metallo-β-lactamases.

2.3. The structure of metallo-β-lactamases

Metallo-β-lactamases are a significant threat to humankind due to their ability to effectively degrade all groups of β-lactam antibiotics, including also Carbapenems. The secondary structure of the B1 subclass of metallo-β-lactamases contains 12 β-sheets and 6 α-helices. These secondary structures are arranged in a four-layer αβ/βα-fold that forms the active center, with two zinc ions, coordinating three amino acids each. His120, His122, His189, and Cys208, His250, Asp124 (amino acids numbering given for NDM-1) are the amino acids involved in zinc coordination.[39] The active site is surrounded by two important loops, namely loop3 (L3, blue circle) and loop10 (L10, red circle), which interact with the substance bound to the active site (Figure 4). The L3 hairpin contains residues offering hydrophobic interaction sites with the hydrophobic parts of a ligand, whereas L10 contains residues capable of forming hydrogen bonds. Some amino acids vary between various B1 metallo-β-lactamases, but in all cases, the flexibility of the loops influence the surface area (i.e. for NDM-1 approx. 520 $Å^2$, where VIM-2 approx. 450 $Å^2$)[40] of the binding site. This flexibility provides a better capacity to bind a variety of antibiotics and hydrolyze them, increasing the spectrum of resistance towards antibiotics.[41]

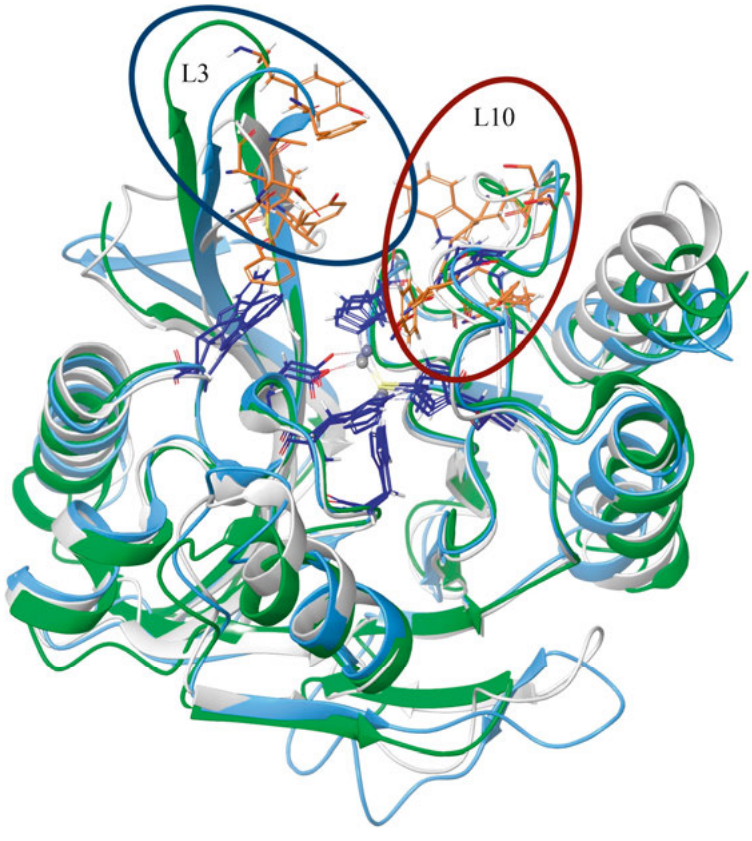

Figure 4. Superimposed binding sites of NDM-1 (cyan), GIM-1 (green), and VIM-2 (grey), with identical AAs shown in blue, and different AAs shown in orange.

2.4. Known metallo-β-lactamases inhibitors

Over the past 14 years, there have been many investigations of the structure and mechanism of NDM-1. Despite these efforts, there are only two compounds in the early clinical trial stage and none in clinical use.[42] The common strategy is to perform structural changes to decrease the hydrolyzing ability of the bacterial enzymes to β-lactam antibiotics. However, the high plasticity of MBL's binding site on the level of the zinc center and on the adjacent substrate-binding loops (Figure 4) results in obstacles for rational drug design strategies as these allow easy adjustments of the binding site size and of the interactions involved in substrate binding.[43]

The small molecules known to bind MBLs can be clustered according to their structural features.[44] The compounds of highest importance are the chelating agents, the covalent inhibitors, and the compounds coordinating zinc ions.

Chelating agents lack selectivity and bind multiple metalloproteins in the human body, and therefore are more toxic whereas covalent inhibitors include cyclic and acyclic boronates that were proven as good inhibitors (Figure 5).

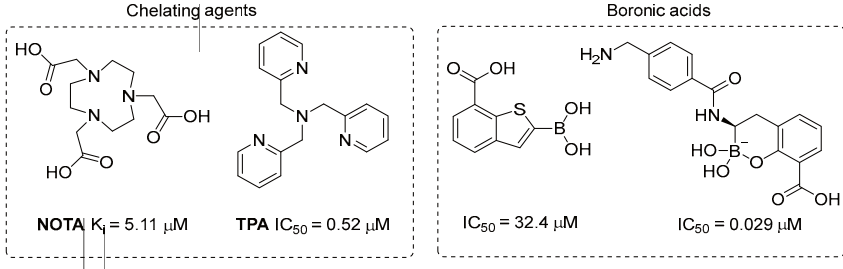

Figure 5. Examples of chelating agent and boronic acid-type inhibitors, with their inhibitory activity being highlighted.

For zinc coordinating inhibitors, the most commonly used reference compound is Captopril, which is weakly active towards MBLs. Although L-Captopril is a stronger inhibitor of NDM-1 than D-Captopril, there is no crystallographic data for it in complex with an MBL. A few interactions have been reported to be important for the binding of D-Captopril to NDM-1, including a hydrogen bond formed with Asn220, coordination to both zinc ions through a thiol, and hydrophobic interactions with Trp93, His249, and Val73 (Figure 6).[45]

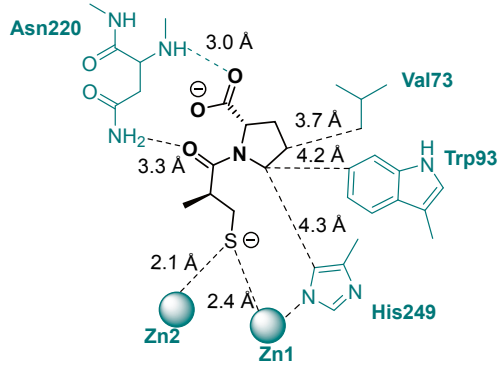

Figure 6. The binding of D-Captopril in the active site of NDM-1 (PDB ID: 4EXS[46]) (Reprinted with permission from ACS Omega **2022**, *7* (5), 4550–4562. Copyright 2022 American Chemical Society).

Captopril is a common starting point for the design of potential MBL inhibitors. Frequently the corresponding thiol group and the carboxylic acid are kept as the thiol can coordinate the zinc ions and the carboxylic acid can serve as a hydrogen bond acceptor. In addition, a hydrophobic part that can interact with L3 is a common motif in the design. Compounds showing a high potency

against MBLs and a binding mode close to that of penicillin have also been shown to be good starting points.

In 2014, a series of 3-mercapto-2-methylpropanoyl amides were reported by Li *et al*.[47]. The goal of this series was to identify the pharmacophore by simplifying the structure of Captopril. The most potent inhibitor of the series had Captopril's proline residue replaced with a benzyl amide or *o*-hydroxylbenzylamide (Figure 7; **1**,**2**). Additional studies showed that the *R* enantiomer of 3-mercapto-2-methylpropanoic acid is the more potent inhibitor than *S* enantiomer (Figure 7, **1**).

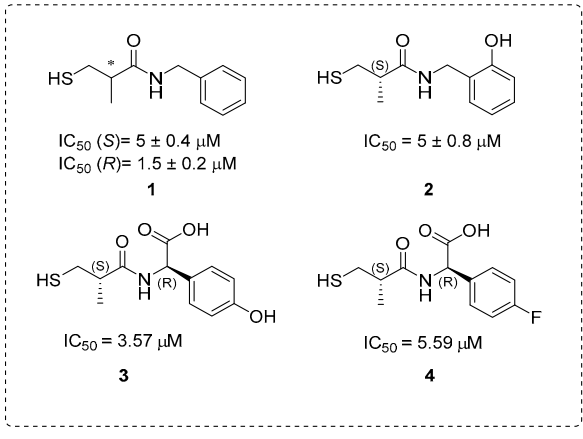

Figure 7. The 3-mercapto-2-methylpropanoic acid derivatives **1**, **2** and the ((*S*)-3-mercapto-2-methylpropanamido) acetic acid derivatives **3** and **4**, along with their activities.

Additional studies were published in 2018 and presented a series of 2-substituted (*S*)-3-mercapto-2-methylpropanamido-acetic acid derivatives, with various amide substituents attached to the carboxylic acid in the α-position to the amide. These compounds were effective against NDM-1 (Figure 7, **4**).[48] VIM-2 was crystallized with both inhibitors, providing valuable structural information. Superimposition of the structure of NDM-1 in a complex with a) hydrolyzed benzylpenicillin and with b) hydrolyzed cephalosporin, similar interactions were observed. In both cases, the carboxylic acid of the ligand formed electrostatic interactions with Lys224 in VIM-2 (Arg228 in NDM-1), and the coordination of **3** and **4** to the zinc ions were similar to that observed for benzylpenicillin and hydrolyzed cephalosporin. This suggested that the structure of hydrolyzed antibiotics may provide useful information in the design of MBL inhibitors.

In 2018, Büttner et al[49] reported a series of Captopril bioisostere thiol-derivatives. In these compounds the methyl group at the β-position to the thiol was replaced

by various aromatic substituents, and the structure of the pyrrolidine ring was varied (Figure 8). The substitution of the methyl group with a benzyl group yielded two-fold increase in inhibition of NDM-1. Modifications of the pyrrolidine ring further improved the activity, as compared to Captopril. The most successful modification was the ring expansion to the corresponding *o*-carboxylpiperidine (Figure 8, **6**). This increased the potency towards NDM-1, VIM-1, and IMP-7 approximately ten times. Further ITC (isothermal calorimetry) studies of **6** in comparison with **7** did not show correlation between IC_{50} and binding enthalpy. Despite different enzyme activity of both compounds had comparable K_d (obtained from ITC measurement), although binding enthalpy was having significantly higher contribution into binding energy of compound **7**. The importance of orthogonal control of thiol-based MBL inhibitors was pointed out due to the enthalpically driven binding of **7** which could be a good starting point for hit to lead process.

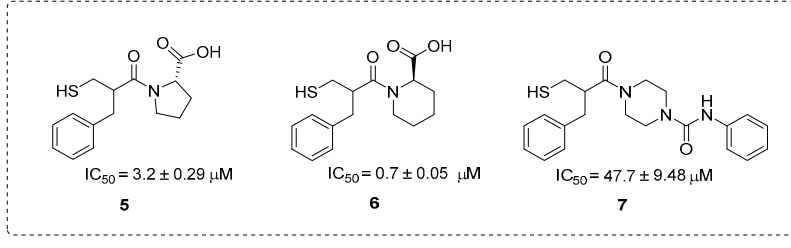

Figure 8. 2-Benzyl-3-mercaptopropionic acid derivatives with inhibition potency against NDM-1.

Ma et al. used a different approach in 2015 to identify MβL inhibitors.[50] They implemented a target-based whole-cell screening assay with ^{1}H NMR spectroscopic detection. This was seen as a method that combines the advantages of target-based and whole-cell screening approaches. The most potent inhibitor identified with this technique was compound **8** (Figure 9), which incorporates an L-tryptophan substituent.

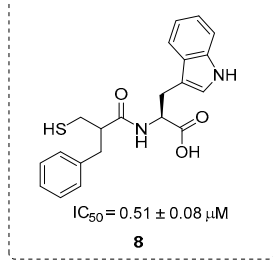

Figure 9. (2-Benzyl-3-mercaptopropanoyl)-L-tryptophan with inhibition potency against NDM-1.

Based on *in silico* fragment-based design, Cain et al.[51] proposed a series of thiols, which showed broad spectrum activity against B1subclass MBLs. The binding of 4-(3-chlorophenyl)-2-(sulfonylmethyl) benzoic acid (Figure 10) to NDM-1 was investigated *in silico*, and to VIM-2 crystallographically. The compound showed a similar binding mode in complex with both enzymes. As expected, the thiol group coordinated the zinc ions, and the aromatic ring was involved in π–π interaction with Trp93 in both NDM-1 and VIM-2.

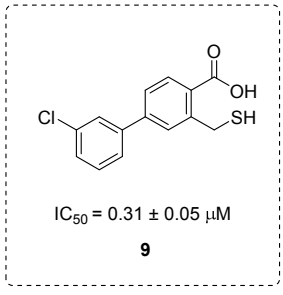

Figure 10. 4-(3-Chlorophenyl)-2-(sulfonylmethyl) benzoic acid **9** and its NDM-1 inhibitory potency.

In 2017, Skagseth et al.[52] synthesized a series of mercapto-carboxylic acid analogues (Figure 11) with the carboxylic acid being replaced by three different bioisosteric groups, namely a phosphonic acid, a phosphonate ester, and a tetrazole. The chain length of the phenylalkyl substituent was explored, as a part of the evaluation of the role of hydrophobicity for bioactivity. In addition, the acetyl-protecting group on the thiol was modified. A broad spectrum of modifications in this series provided improvement in NDM-1inhibition.

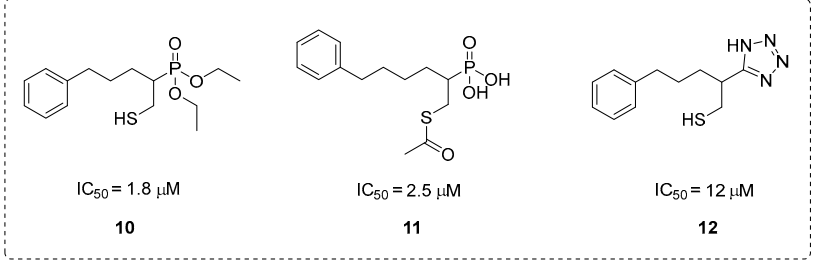

Figure 11. Carboxylic acid bioisosteres and their NDM-1 inhibition potencies.

The compounds containing a thiol, or its protected version, and a phosphonic acid/ester showed the best inhibitory activities. Compounds **10** and **11** were successfully crystallized with VIM-2 delivering information about their binding modes. It is clearly seen in theses crystal structures that the thiol, or its protected analogue, coordinated to zinc ions and the phosphonate group

formed a hydrogen bond to Asn233. All compounds showed better activity towards VIM-2 than towards NDM-1. The comparison of the crystal structure of **12** with VIM-2 and the computed structure of **12** with NDM-1 suggested that the weaker hydrophobic interaction of **12** with NDM-1 could explain the difference in activity.

3. Overview of methods

3.1. Enzyme assay

One of the commonly used parameters to determine drug efficacy is the half-maximal inhibitory concentration (IC_{50}). It gives information about the quantity of the drug necessary to inhibit a process to a 50% extent. All synthesized compounds we evaluated against NMD-1, VIM-2, and GIM-1 in enzyme assays, majority of the studies was done by Skagseth Susann at UiT. The inhibitory activities were assessed in the presence of Nitrocefin (for VIM-2 and GIM-1) and Imipenem (for NDM-1) through UV-Vis absorption with maximum absorption at 480 nm, and 300 nm, respectively.[53] These compounds (Figure 12) are commonly used in β-lactamase assays, due to their susceptibility to β-lactam ring hydrolysis and to their UV-Vis absorbance.

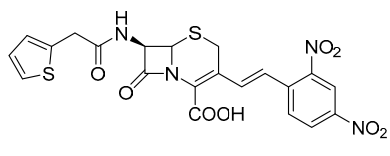

Nitrocefin

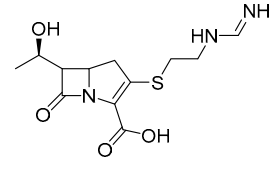

Imipenem

Figure 12. Structures of the reference compounds used for biological assays with MBLs.

Each of the potential inhibitors were tested in triplicates. The inhibitor concentration dependence of the UV-Vis absorption was fitted to a competitive inhibition model,[53-54] plotting the % inhibition as a function of the logarithm of the inhibitor concentration (Figure 13).

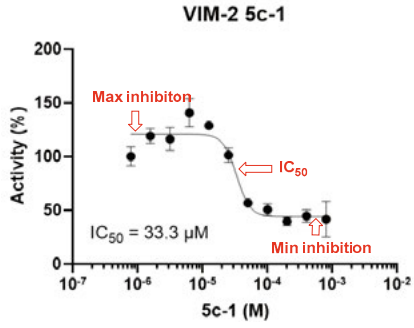

Figure 13. An activity versus concentration plot, used to determine IC_{50} values (used example of the plot comes from SI of Paper II).

3.2. Protein backbone assignment

As 2D NMR experiments become insufficient to study proteins larger than 10 kDa, 3D and 4D NMR spectroscopic methods have been established. Backbone resonance assignments of large proteins (> 150 residues) demand the fulfilment of certain requirements. Experiments recorded for backbone assignments are time consuming and therefore the studied protein should be stable and should typically be $^{2}H/^{13}C/^{15}N$ isotope labelled. A general recommendation is to use ^{13}C and ^{15}N isotopes for proteins smaller than ~30 kDa, and implement ^{2}H isotope labelling for larger proteins. To compensate for the slow tumbling induced quick T_2 relaxation, raising the temperature may compensate to a certain extent. NDM-1 is a challenging protein as it is unstable. Accordingly, ten years following its discovery, only a few NMR studies of NDM-1 have yet been published. In our hands, NDM-1 was stable over two weeks at 25 °C, and for four days at 37 °C. To achieve the full assignment of the unstable protein, targeted acquisition (TA) and non-uniform sampling (NUS) was needed. These methods allow for recording high-quality spectra in a shorter time than using standard experiments. Backbone resonance assignment was performed using 2D $^{1}H,^{15}N$ HSQC and HNCA (hncagpwg3d)[55], HN(CO)CA (hncocagpwg3d)[55], HNCACB (hncacbgpwg3d)[56], HN(CO)CACB (hncocacbgpwg3d)[57], HNCO (hncogpwg3d)[55], and HN(CA)CO (hncacogpwg3d)[58] spectra through TA and NUS. The information content of each is summarized in Table 1 and Figure 14. The general strategy of the assignment is described below. For proteins larger than 50 AA, ^{2}H labelling is typically necessary. This was not required for NDM-1.

Table 1. Overview of run protein backbone experiment (based on [59]).

Protein labelling	Experiment	Information
^{15}N and ^{13}C	**3D** HNCO	amino acids sequence connection for the backbone (^{13}C'=O chemical shift)
	3D HN(CA)CO	
	3D HNCA	amino acids sequence connection for the backbone (^{13}Cα chemical shift)
	3D HN(CO)CA	
	3D HNCACB	amino acids sequence connection for the backbone (^{13}Cα & ^{13}Cβ chemical shift)
	3D HN(CO)CACB	
^{15}N	**2D** ^{1}H-^{15}N HSQC	^{1}H chemical shift of amide proton

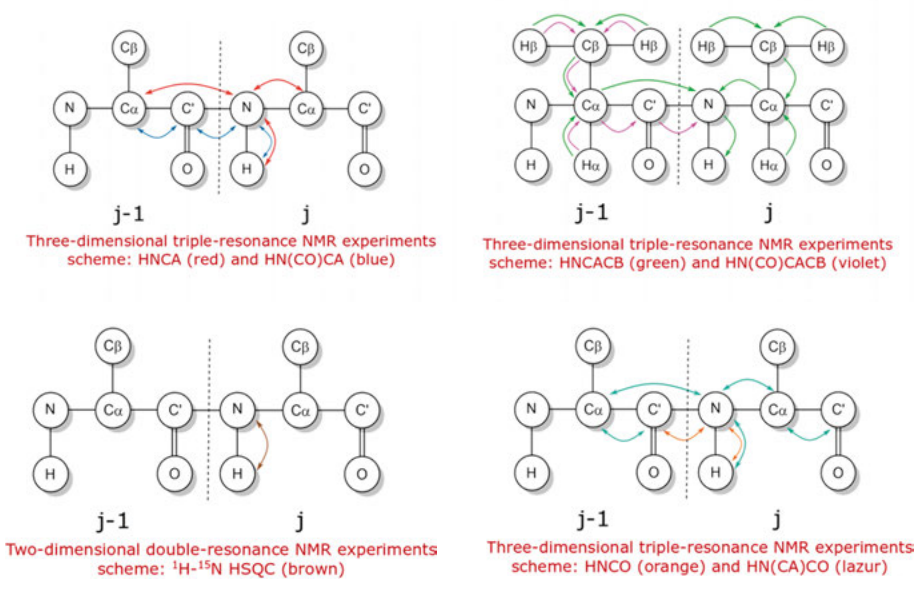

Figure 14. Graphical representation of the 3D experiments used for NDM-1 assignment.

Backbone sequence assignment: From the HNCACB spectrum, the starting point of the assignment is identified since the average chemical shifts of Cα and Cβ are specific for each amino acid (Figure 15). The most characteristic signals are those Glycine, Alanine, Serine, and Threonine. For Gly, the chemical shift of Cα is around 45 ppm and it does not have a Cβ carbon; Cβ is observed between 15–20 ppm for Ala, which is lower than for all other amino acids; and only for Ser and Thr Cβ has a lower chemical shift than Cα. Thus, these distinctive signals are the best starting points for assignment.

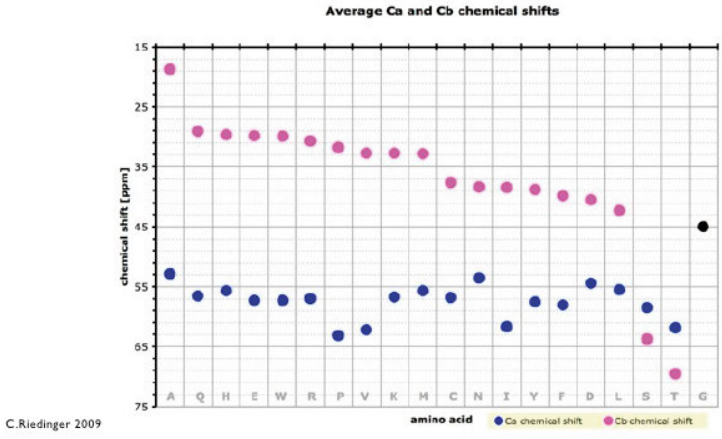

Figure 15. Average chemical shifts for Cα and Cβ of specific amino acids (Picture used with permission of the author from presentation https://www.slideshare.net/shalaree/nmr-assignments-and-structure-determination).

Based on HNCACB and HN(CO)CACB experimental data, the Cα and Cβ of a residue and its neighboring residues, respectively, are identified. For each ^{15}N chemical shift (one strip) HNCACB contains four peaks, Cα and Cβ from the same residue, and the NH group and Cα and Cβ from the neighboring residue. As a next step, based on the HN(CO)CACB experiment, one can identify the Cα and Cβ that belong to the adjacent amino acid (Figure 16).

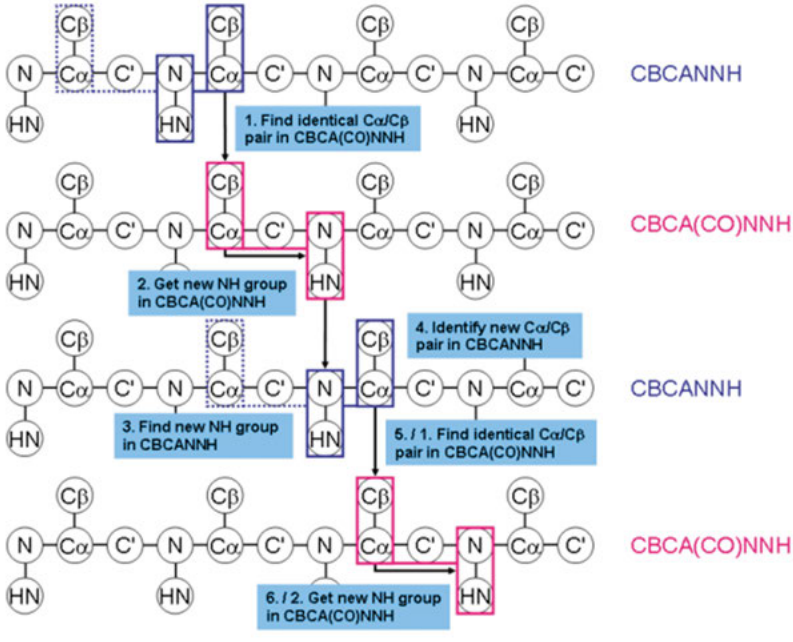

Figure 16. Flow chart of correlation of the NH, based on the preceding Cα and Cβ chemical shifts, using NHCACB and NH(CO)CACB.(Picture used with permission, from website https://www.protein-nmr.org.uk/.)

A similar approach is used while analyzing HNCA and HNCOCA, HNCO, and HNCACO data, with the advantages of using the more sensitive HNCO and HNCA experiments. In this approach, Cα and C' are identified instead of Cβ. Analogous to the previous approach, for each ^{15}N chemical shift (one strip) HNCA contains two peaks, Cα from the residue as the NH group and Cα from the neighboring residue. In the next step Cα that belongs to the adjacent amino acid can be identified based on HN(CO)CA (Figure 17).

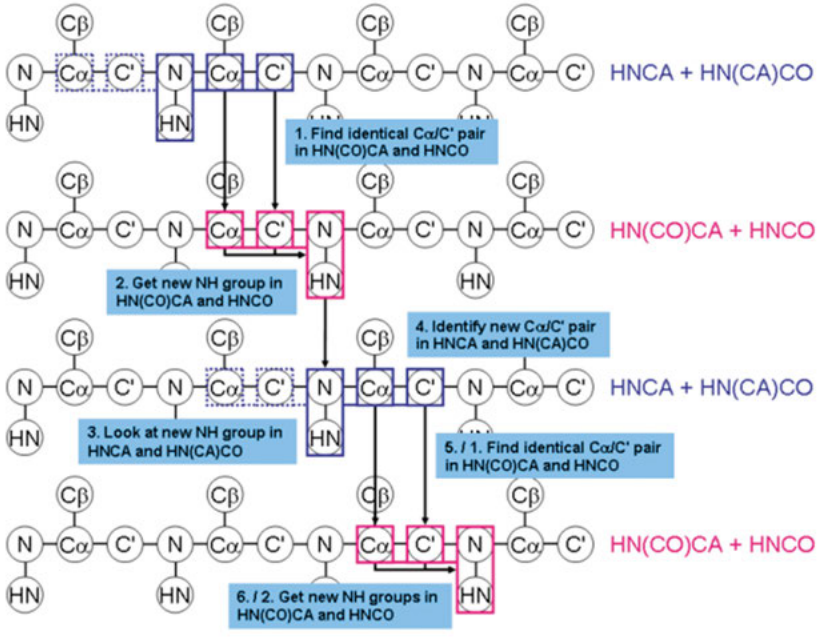

Figure 17. Flow chart of correlation of the NH based on the preceding Cα and Cβ chemical shifts, based on the NHCA and NH(CO)CA.(Picture used with permission of the author from website https://www.protein-nmr.org.uk/.)'

These two methods allow for linking neighboring amino acids. For proteins larger than 200 amino acids, HNCACB and HN(CO)CACB may lose sensitivity, and the Cβ signals might disappear in the noise. The assignment of these is done with an alternative approach, which makes use of the Cα and C' signals instead.

3.3. Chemical shift perturbation

In depth characterization of compounds, such as biophysical characteristics, and protein-ligand interactions are helpful for drug discovery all the way from identifying a starting point to a drug, through identifying a hit to the characterization of clinical candidates. A commonly used technique is X-ray diffraction, where protein-ligand co-crystals are studied to describe the binding interactions. X-ray diffraction provides information on a static structure. Some proteins, such as NDM-1, are not that easy to co-crystallize with ligands. These can be best studied by solution NMR that in addition also provides information on conformational and binding dynamics.

One of the common target-based approaches, which allow the study of binding sites was described by Williamson in 2013 as chemical shift perturbation (CSP).[60] This method uses the chemical shift dependence of a nuclei on its chemical environment. Following changes in the chemical shift on residues involved, binding events and conformational changes can be studied. Using this method, it is possible to identify the position of a ligand binding site, determine the binding affinity, and/or use the chemical shift changes to guided computational docking to determine the binding mode of a ligand. The dynamics of processes, such as binding and conformational exchange, can be classified as fast, intermediate, or slow (Figure 18).

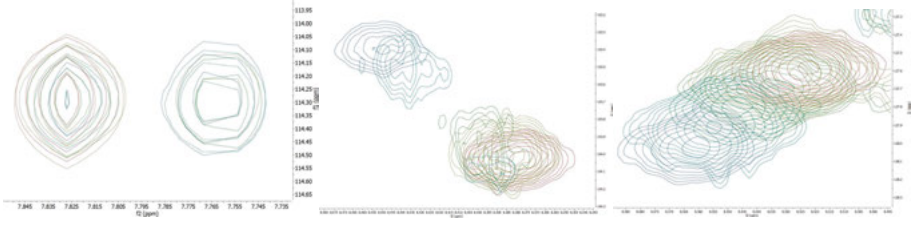

Figure 18. Chemical shift perturbation pattern depends on the exchange rate as compared to the NMR time. Slow, intermediate and fast exchange are shown from the left to the right.

Chemical shift perturbations were calculated according to equation *1*:[60]

$$\mathrm{CSP} = \sqrt{(\Delta\delta_{1H}{}^2 + ({}^1/_{R_{scale}} \times \Delta\delta_{15N}{}^2)} \qquad R_{scale} = 6.5 \quad (1)$$

Where $\Delta\delta_{1H}$ is the chemical shift change for proton dimension, $\Delta\delta_{15N}$ is the chemical shift change for nitrogen dimension, R_{scale} is a scaling factor.

For each AA showing CSP, the dissociation constant can be obtained by fitting the data to the equations *2* or *3*, depending on the exchange rate:[61]

$$\Delta\delta_{obs} = \Delta\delta_{max} \frac{([P]+[L]+K_d) - \sqrt{([P]+[L]+K_d)^2 - 4[P][L]}}{2[P]} \quad (2)$$

$$\mathrm{I}_{obs} = \mathrm{I}_{max} \frac{([P]+[L]+K_d) - \sqrt{([P]+[L]+K_d)^2 - 4[P][L]}}{2[P]} \quad (3)$$

Where K_d is the dissociation constant, I_{obs} are normalized integrals from bound form, I_{max} is the normalized integral for the last titration step, and [P] and [L] are protein and ligand concentrations, respectively. $\Delta\delta_{max}$ were estimated using the software MestReNova, by extrapolation of the binding induced chemical shift differences $\Delta\delta_{obs}$.

In this thesis K_d values were calculated for all amino acids with observed significant shift change, spontaneously. For accurately calculate K_d value, $\Delta\delta_{max}$ and I_{max} would have to be experimentally measured, which often is not possible. Therefore those values are obtained during the curve-fitting, or estimated from last titration step of large acess of ligands. Moreover, protein concentration measurement have certain degree of accuracy. Due to those reasons, spontaneous fitting of multiple titrations curves allows for higher accuracy of the K_d.[60]

3.4. NOESY based experiments

Cross-relaxation allows for the transfer of nuclear spin polarization to another spin-active nuclei through space. This is the so-called Nuclear Overhauser Effect (NOE). NOE-based experiments were proven to be invaluable to study protein-ligand complexes.[62-65] $^{1}H,^{1}H$ NOE correlations help to create a three-dimensional picture of a studied molecular system. This phenomenon can be used both for intra- and intermolecular interactions. To study protein-ligand interactions, isotope-filtered NOESY experiments can be necessary, which selectively provide signals between the labelled protein and the unlabeled ligand, avoiding sever overlaps with protein-protein NOEs. In this thesis work, 2D ^{15}N-filtered NOESYand 3D ^{15}N-filtrated HSQC-NOESY were employed.

The 3D ^{15}N-filtered HSQC-NOESY provides a three-dimensional spectrum with ^{15}N, ^{1}H, and ^{1}H dimensions. As indicated by the pulse sequence's name, the plane of $F_2(^{1}H)$-$F_3(^{1}H)$ represents the NOESY spectrum, and the $F_1(^{15}N)$-$F_2(^{1}H)$ corresponds to a 2D ^{1}H-^{15}N HSQC (Figure 19) .

Figure 19. Graphical representation of HSQC-NOESY and HOESY NMR experiments.

The 2D ^{15}N-filtered NOESY results in a two-dimensional spectrum with two proton dimensions, from the ligand to the protein, where the $F_1(^{1}H)$-$F_2(^{1}H)$ represents the NOESY map.

NOEs are powerful to study intermolecular interactions. Classic $^{1}H,^{1}H$ NOESY for large systems contain a significant amount of signal overlaps. The equivalent of NOESY experiment can be applied for two different nuclei, for example fluorine and proton (named then ^{19}F-^{1}H HOESY). Heteronuclear NOEs help to avoid signal overlaps. In this thesis, heteronuclear NOE (HOE) was detected with magnetization transfer from the heteronucleus (^{19}F) to proton, using a ^{19}F-^{1}H HOESY (Figure 19) experiment.[66] This method can be used for studying interactions, using either ^{19}F-labeled proteins or fluorinated small molecules.

3.5. Molecular docking studies

The 3D structure of a protein-ligand complex can be predicted also by computational methods, referred to as molecular docking. Ideally, this strategy should result in an optimal binding position and orientation of the bound ligand. The easily accessible methods are commonly divided into the following types: *i*) rigid, *ii*) semi-flexible, and *iii*) flexible docking. For the MBLs, with flexible loops surrounding the binding site, whose conformations are changing the shape and size of the binding pocket, the Glide-Schrödinger and Prime – MM-GBSA combination, which is also known as the induced-fit docking approach, was chosen (Figure 20).

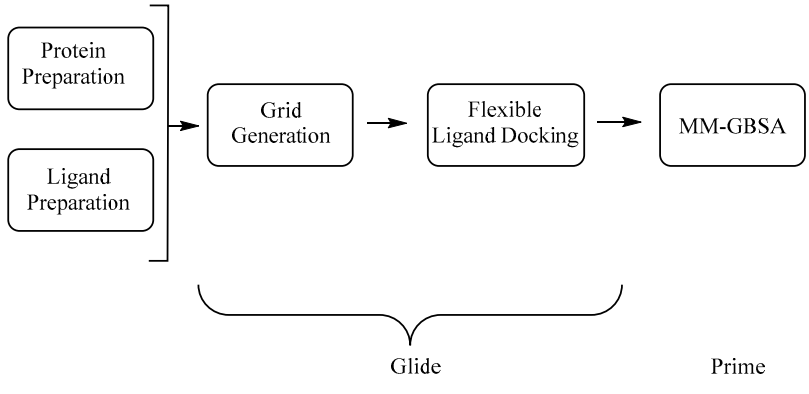

Figure 20. Steps taken during a molecular docking procedure.

Primarily, certain requirements for the ligand and the receptor have to be fulfilled, to perform ligand docking. In the case of the ligand, different protonation, tautomeric stages, and enantiomers are sampled and generated accurately, and minimized, based on the energy of 3D structures.[67] Accordingly an X-ray structure might have some flaws, which is supposed to be fixed to obtain the best results by docking. Primarily, a PDB structure with at least 2.5 Å resolution should be used. Moreover, the protein preparation process (Protein

Prep Wizard) is used to resolve structural uncertainties, like protonation/tautomerization of histidine, distinguishing oxygen and nitrogen in Asn or Gln, and/or carbon and nitrogen atoms in the imidazole ring of His. In other words, all atoms, bond orders, and formal charges should be correct.

Having prepared the receptor and ligands properly, a docking grid is generated, within which Glide can search for favorable interactions. Determination of the grid box is a key step that can significantly influence the docking results. In this case, no constraints were implied to avoid forced docking, with a high energy penalty. When the generated ligand set has been docked, to the rigid receptor structure, and a Prime MM-GBSA calculations are performed (Molecular mechanics with generalized Born and surface area solvation), which generates free binding energies according to equation (*3*).

$$\Delta G_{(bind)} = E_{complex(min)} - (E_{ligand(min)} + E_{protein(min)}) \quad (3)$$

At the end of the process, the docked poses with the most overlap between NMR and molecular docking were proposed as the most reliable predictions.

4. New metallo-β-lactamase inhibitors

Although the MBL inhibitors discussed in Chapter 2.4 cover a wide range of substances, so far only two have reached clinical trials. MBLs keep on mutating (currently 806[68]) and the resistance genes are spreading, further worsening the antibiotic resistance crisis. Motivated by the acute necessity of finding clinically applicable MBL inhibitors this thesis work focused on the design, synthesis and structural studies of new potential MBL inhibitors (MBLIs). Chapters 4.1 and 4.2 describe the evaluation of inhibitors containing phosphonamidates and phosphonic acid moieties (both containing P=O), respectively. (Figure 21) Phosphonic acids are more acidic (pK_a ~1-3) and more polar than carboxylic acids, and therefore are expected to show improved aqueous solubilities as compared to carboxylic acids.[69] Additionally, phosphonic acids in contrast to carboxylic acids are nonplanar, which is expected to be of advantage for drug development,[70] nonetheless for mimicking the transition state of β-lactam antibiotic hydrolysis by MBLs.

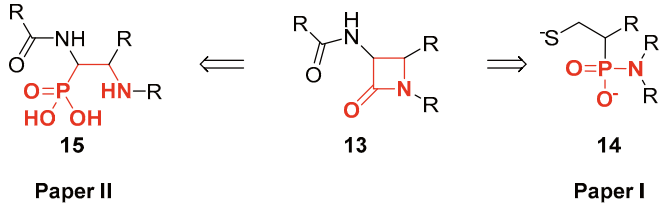

Figure 21. The core structures of inhibitors mimicking the tetrahedral intermediate, and their phosphonamidate and phosphonic acid analogues.

Chapter 4.3 describes the NMR-based structural study of fluorine substituted Captopril analogues. These allow the use of ^{19}F NMR in the investigation of their protein binding, promoting structural studies, and thereto are expected to have somewhat lower pK_a and thus higher aqueous solubility when compared to non-fluorinated thiols. They admittedly have a further key advantage, which strategy is unpublished yet and therefore cannot be discussed herein.

4.1. Phosponamidate-based MBL inhibitors (Paper I)

Our design was inspired by the structure of existing antibiotics and MBL inhibitors (Figure 22).

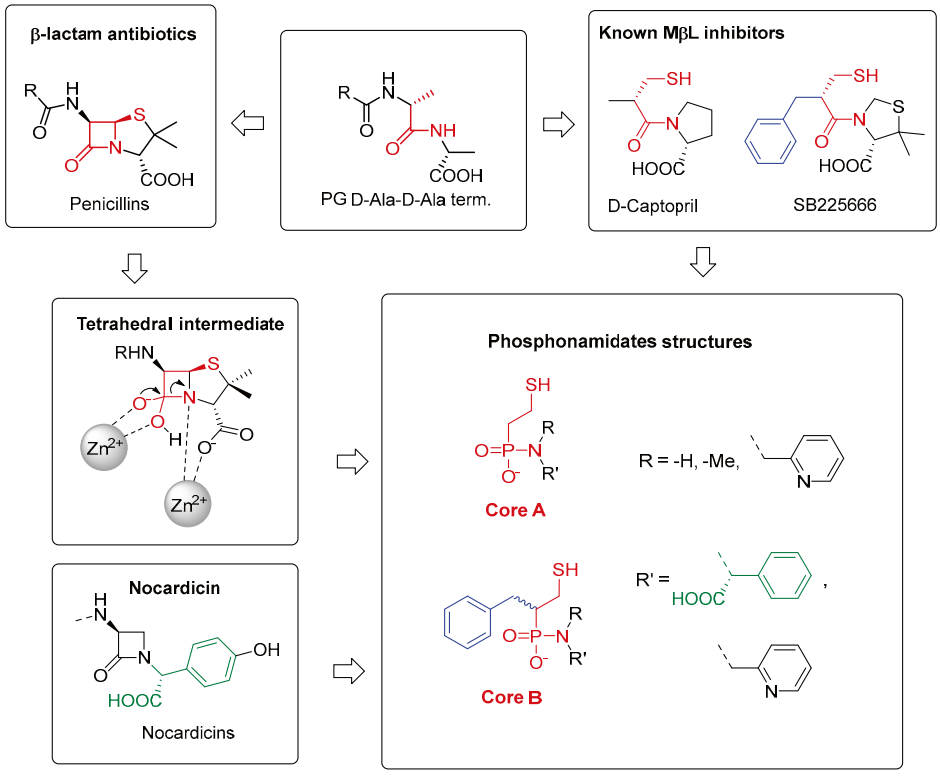

Figure 22. The design of phosphonamidate-type MBL inhibitors. [71]

Keeping in mind the geometry of the tetrahedral transition state of β–lactam hydrolysis (Figure 3, Chapter 2.2), a phosphonamidate was incorporated. This has a tetrahedral geometry and it is expected to be hydrolysis resistant as compared to a β-lactam amide. The phosphoamidate motif was used to design phosphorous analogues for D-Captopril[72] and SB225666,[73] preserving the pyrrolidine or thiazolidine rings and an amide bond. A 2-mercaptoethyl moiety was further introduced to increase binding affinity.[45] (2-Mercaptoethyl)phosphonamidates (*Core A*) and (1-mercapto-3-phenylpropan-2-yl)phosphonamidates (*Core B*) were selected as core structures. As the synthesis of phosphonamidates with a cyclic amine component bound to the phosphorus was troublesome, noncyclic secondary and primary amines were instead applied. The structure of the designed compounds resemble the analogues of the monobactam Nocardicin. These have a β-lactam ring substituted with a 2-(4-hydroxyphenyl)acetic acid.

To obtain phosphonamidate inhibitors, the essential step was the coupling of a phosphonic monoacid and an amine. This step (Figure 23c and 24e) required extensive optimization, and the product was finally obtained when using triphenylphosphine dichloride, PPh_3Cl_2, as the catalyst. In the model synthesis, *S*-(2-(hydroxy(methoxy)phosphoryl)ethyl)ethanethioate and *S*-(2-(hydroxy(methoxy)phosphoryl)-3-phenylpropyl)ethanethioate were used as core structures and are here denominated as *Core structures A* and *B*, respectively.

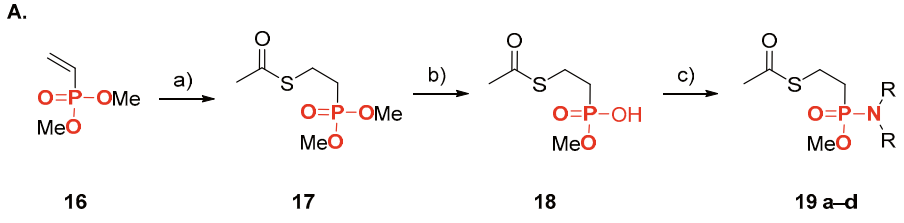

Figure 23. Reagents and conditions: **A.** a) thioacetic acid, $CHCl_3$, 60°C, 7 days, 51%; b) NaI, acetone, 60 °C, o.n., 68%; c) selected amine, PPh_3Cl_2, Et_3N, DCM, r.t., Ar, o.n., 13-86%.

The sulfa-Michael addition of dimethyl vinylphosphonate **16** and thioacetic acid in chloroform yielded **17**, by the condensative formation of a new C-S bond. Alternatively, the reaction was run with potassium thioacetate, although this resulted in a lower yield. Upon monohydrolysis of the phosphonic ester of **17** using sodium iodide, compound **18** was obtained. To obtain phosphonamidates, the common peptide synthesis coupling reagents COMU/Oxyma, PyAOP, PyBOP, HATU, HOBt, oxalyl chloride, and thionyl chloride were tested; however, without success. Most of these reactions led to the formation of monophosphonic acid anhydride. Successful conversion to the phosphonamidate was obtained in a PPh_3Cl_2-mediated reaction, in which the hydroxyl group was first converted into a more reactive phosphonium ylide, and a subsequent nucleophilic attack by the amine resulted in $O{=}PPh_3$ elimination and simultaneous formation of a P-N bond.

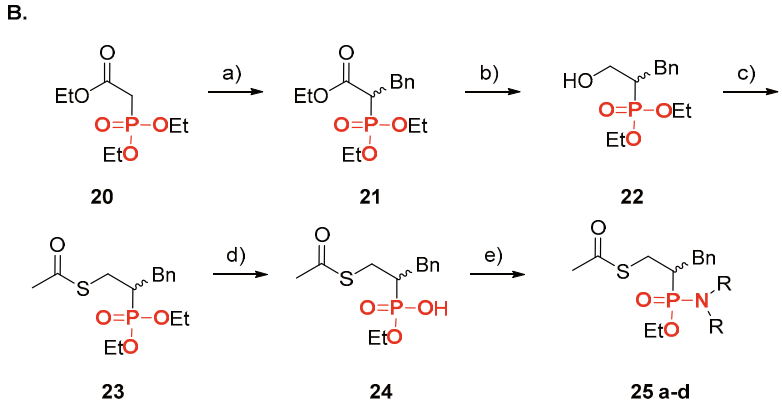

Figure 24. Reagents and conditions: **B.** a) benzyl bromide, NaH, dry DME, 0 °C to r.t., o.n., 41%; b) 2M $LiBH_4$ in THF, -20 ° C to rt, o.n., 91%; c) thioacetic acid, DEAD, PS-PPh_3, dry THF, -5 °C to r.t., on, 59%; d) LiBr, 2-butanone, 80 °C, o.n., 96%; e) NH-RR', PPh_3Cl_2, Et_3N, DCM, r.t., Ar, o.n. 19-96%.

The synthesis of phosphonamidates possessing *Core B* (Figure 24) required five steps: a coupling of the phosphonic monoacid and an appropriate amine, the selective monohydrolysis of a methyl ester, a Mitsunobu reaction, a reduction of an ester to an alcohol, and monoalkylation of the triethylphosphonoacetate. The first step was optimized to obtain the best ratio between product **21** and the dialkylated byproduct (3:1), using NaH as base. In the next step, the ethyl ester was reduced to the primary alcohol **22** with $LiBH_4$ in THF, which was subsequently converted into thioester **23** under typical Mitsunobu conditions with DEAD, and solid-supported PS-PPh_3. The latter was used to avoid troublesome purification of the O=PPh_3 side product. The last two steps were analogous to those of the synthesis of *Core A*. However, the hydrolysis of the ethoxy group using LiBr in butan-2-one (Figure 24d) provided higher yield as compared to that mediated by NaI in acetone (Figure 23b). Using these two synthetic pathways eight compounds were synthesized (Figure 25).

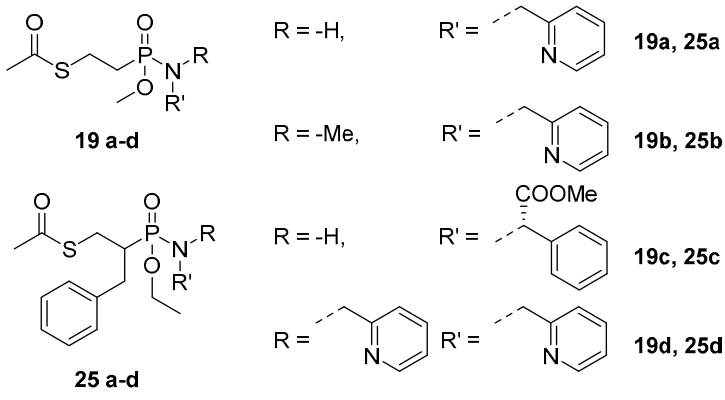

Figure 25. Phosphonamidates synthesized as MBL inhibitory candidates.

4.2. Phosphonic acid-based MBL inhibitors (Paper II)

Whereas the C(=O)-N (lactam) analogue P(=O)-N amide is conserved in the phosphonamidates above, the phosphonic acid derivatives developed below better mimic the transition state of the β-lactam hydrolysis. A series of twelve phosphonic acid derivatives were synthesized (for a detailed description of the synthesis, see paper II), and were then studied as twenty-four compounds following chromatographic separation of the diastereomer pairs (Figure 26).

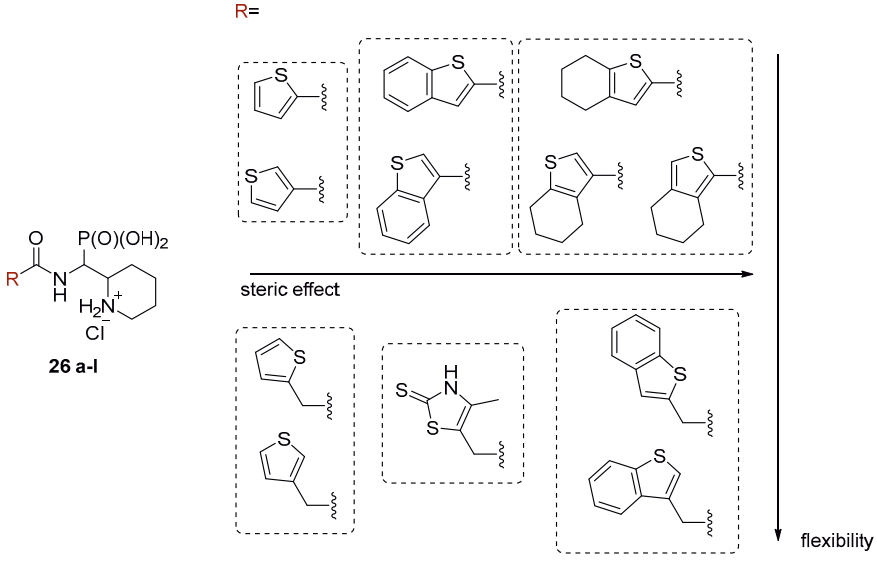

Figure 26. The piperidine substituted phosphoester-type MBL inhibitors.

In this series of compounds, we explored the influence of aromatic groups, such as thiophenes and (thiophene-2-yl)acetamides, which are bioisosteres of phenyl and benzyl groups, respectively. The amide substituents were chosen to allow us to study the influence of regioisomerism, steric effect, polarity and flexibility on the inhibitory activity. Additionally, all the substituents were more polar than their bioisosters, which was expected to be beneficial for their aqueous solubility.

4.3. Fluorine-labelled MBL inhibitors (Paper III)

In collaboration with Prof. Annette Bayer at Tromsö University, the MBL binding of fluorine labelled 3-mercapto-2-methylptopanoic acid analogues (Figure 7; **1** in Chapter 2.4) was studies by NMR (Figure 27). The purpose of the compound series was to use the ^{19}F-^{1}H HOESY experiment to obtain more information about the binding site, without the need for ^{19}F protein labelling.

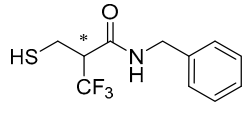

28

rac (**28**) IC_{50}=31μM
E1 (**28-1**) IC_{50}=10μM
E2 (**28-2**) IC_{50}=75μM

Figure 27. Fluorine-containing inhibitors with their inhibitory activity against NDM-1.

5. Metallo-β-lactamase binding

5.1. Metallo-β-lactamase inhibitory activity

To determine the activity of the synthesized compounds, their half-maximal inhibitory concentration (IC_{50}) against NDM-1, GIM-1, and VIM-2 were measured in an enzymatic assay (Details can be found in Chapter 3.1), and results were summarized below (Figure 28). Detailed information can be found in Paper I in the section *MBL inhibition assay*.

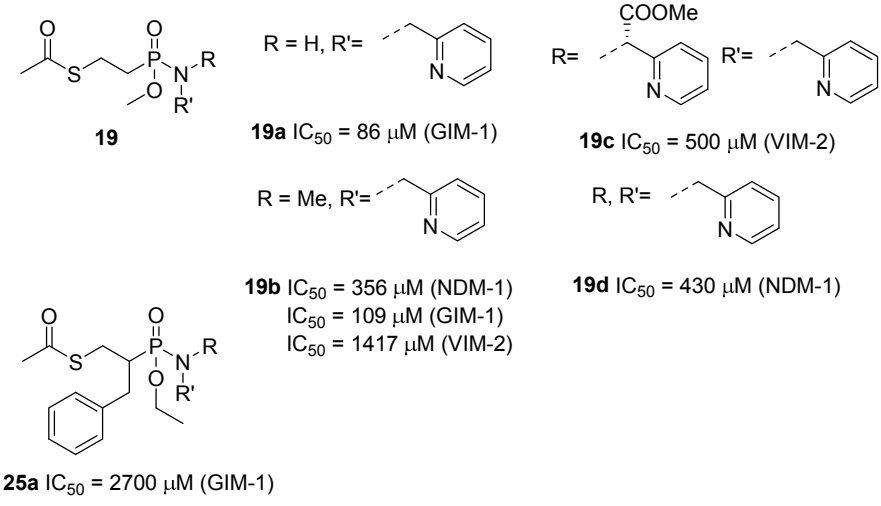

Figure 28. The inhibitory activity of the phosponamidate-based compounds against NDM-1, GIM-1, and VIM-2.

Five of the phosphonamidates (Chapter 4.1) showed activity against at least one of the tested MBLs. Compounds **25** possessing *Core B* and hence containing a hydrophobic benzyl sidechain showed low aqueous solubility, preventing the evaluation of their MBL inhibitory activities. Compounds **19a–d**, which possess *Core A* and do not have a phenyl group showed medium activities (up to 86 μM). Additionally, inhibitory essay in *E.coli* in presence of meropenem and cytotoxicity against HeLa cells were performed, and resulted with no significant activity.

We tested the α-aminophosphonic acid derivatives (Chapter 4.2) for inhibitory activities against the same three enzymes, with their IC_{50}s being shown in Figure 29.

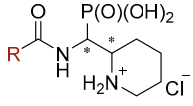

26 a-l

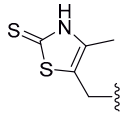

26a-1 *SR/RS*
IC_{50} = 353 μM (VIM-2)

26b-1 *SR/RS*
IC_{50} = 230 mM (NDM-1)
IC_{50} = 661 μM (GIM-1)
IC_{50} = 118 μM (VIM-2)
26b-2 *RR/SS*
IC_{50} = 7.2 μM (VIM-2)

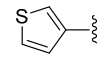

26c-1 *SR/RS*
IC_{50} = 219 μM (NDM-1)
IC_{50} = 33 μM (VIM-2)
26c-2 *RR/SS*
IC_{50} = 33 μM (VIM-2)

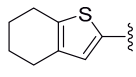

26d-1 *SR/RS*
IC_{50} = 244 μM (VIM-2)
26d-2 *RR/SS*
IC_{50} = 4.5 μM (VIM-2)

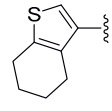

26e-1 *SR/RS*
IC_{50} = 76 mM (NDM-1)
IC_{50} = 69.7 μM (VIM-2)
26e-2 *RR/SS*
IC_{50} = 46.1 μM (VIM-2)

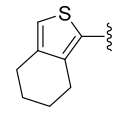

26f-1 *SR/RS*
IC_{50} = 121 μM (GIM-1)
IC_{50} = 37 μM (VIM-2)
26f-2 *RR/SS*
IC_{50} = 18.8 μM (VIM-2)

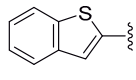

26g-1
IC_{50} = 46.7 mM (NDM-1)
IC_{50} = 45 μM (VIM-2)
26g-2
IC_{50} = 46.8 mM (NDM-1)
IC_{50} = 4.1 μM (VIM-2)

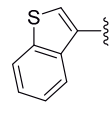

26h-1 *SR/RS*
IC_{50} = 228 mM (GIM-1)
IC_{50} = 69.7 μM (VIM-2)
26h-2 *RR/SS*
IC_{50} = 11.6 μM (VIM-2)

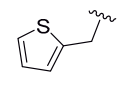

26i-1
IC_{50} = 296 μM (NDM-1)
26i-2
IC_{50} = 271 μM (NDM-1)
IC_{50} = 328 μM (VIM-2)

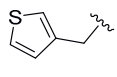

26j-1 *SR/RS*
IC_{50} = 506 mM (NDM-1)
IC_{50} = 319 μM (VIM-2)

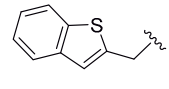

26k-1 *SR/RS*
IC_{50} = 56.6 mM (NDM-1)
26k-2 *RR/SS*
IC_{50} = 22.4 mM (NDM-1)
IC_{50} = 17.1 mM (GIM-1)
IC_{50} = 28.7 μM (VIM-2)

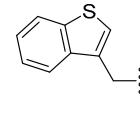

26l-1 *RR/SS*
IC_{50} = 7.9 μM (NDM-1)
26l-2 *RS/SR*
IC_{50} = 27.8 μM (NDM-1)
IC_{50} = 94.4 μM (VIM-2)

Figure 29. The inhibitory activity of the α-aminophosphonic acid-type compounds against NDM-1, GIM-1, and VIM-2.

Out of the twenty-four compounds, twenty-two showed activity against at least one MBL, with **25d-2** and **25g-2** showing the highest activities, 4.5 and 4.1 μM, respectively, against VIM-2. (Details including all results can be found in Paper II in the section *Metallo-β-lactamase Inhibition and Cytotoxic Activities*.) It should be noted that almost all synthesized compounds inhibited VIM-2 whereas only a lesser number inhibit NDM-1 and GIM-1. Preferences of stereochemistry was observed. For NDM-1 better activity usually was observed by compounds with SR/RS configuration, and for VIM-2 with RR/SS configuration. Compounds lacking a flexible methylene between their amide and aromatic moieties showed best affinities. Increased flexibility led to up to a tenfold activity decrease for compounds having 2-thiophene or 3-thiophene rings. None compound was detected to be cytotoxic against HeLa cells.

The fluorine-labelled inhibitors, discussed in Section 4.3 were tested for activity against NDM-1 (Figure 27). As the *S*-acetyl-protected compounds did not show inhibitory activity against NDM-1, the acetyl group was removed. The corresponding free thiols showed activity, IC_{50} 31 μM, as an enantiomeric mixture, and the separated enantiomers showed IC_{50} 10 μM and 75 μM, respectively. As a control experiment, TCEP, which was used to reverse spontaneous disulfide formation[74], was tested against NDM-1 and did not show any NDM-1 inhibition.

5.2. Protein-ligand interactions - studied by NMR

NMR spectroscopy is an important tool for drug discovery. It provides complementary information to other biophysical methods about biological systems, such as an understanding of dynamic processes that are not possible to study with X-ray crystallography, for example. Ligand-observed and the target-observed techniques are the two main NMR approaches in drug discovery.[75] Ligand-based methods, in which the ligand but not the protein signals are assessed, have the advantage that no expensive and often challenging labelling of protein is necessary. It requires smaller quantities of the target protein, and thereto the simplicity of the spectra makes the analysis easier. These techniques are often used in screening. Target-observed approaches are used, for instance, to identify the binding site of ligands, gain information on changes in protein dynamics upon ligand binding, and determine binding affinity.[76-77] In this thesis, target-observed methods were used. The chemical shift perturbation (CSP) of protein ^{1}H and ^{15}N nuclei, ^{15}N-filtered HSQC-NOESY, and $^{1}H,^{19}F$ HOESY were applied to identify the binding site and mode of the inhibitors. Target-based approach NMR studies necessitate the backbone assignment of the protein of interest. Here, two proteins were studied,

NDM-1 and VIM-2.The assignment of NDM-1[78-80] was performed as part of the work, whereas for VIM-2 a literature assignment was made use of.[81]

To test the stability of NDM-1, two batches of 250 µM protein were kept at 25 °C and 37 °C for two weeks, acquiring $^{1}H,^{15}N$ HSQC spectra every 24 hours. The protein was stable for two weeks at 25 °C, whereas at 37 °C protein degradation was observed after four days. As a better resolved $^{1}H,^{15}N$ HSQC spectrum was obtained at 37 °C,[82] the spectra for assignment and for detection of inhibitor binding were detected at this temperature with changing the sample every 4 days.

The backbone of the NDM-1 was assigned based on multiple 3D NMR spectra, as described in detail in Chapter 6.2, achieving 88% assignment for the backbone ^{1}H ^{15}N residues (excluding the prolines; Figure 30): The amino acids Gly36-Met39, Gly69, Ala72, Gly84, Lys106-Iso109, Lys125, Met126, Ala165, Gly178, Gly186, Gly207, Cys208, Lys216-Leu221, His250, and Arg251 remained unassigned, due to peak broadening or peak overlaps. In addition, 89% of the backbone carbonyl carbons (Figure 31), and 91% of the C_α and C_β resonances were assigned.

In parallel to this work, Yao et al assigned 84% of the residues of the NDM-1 backbone (excluding prolines),[80] with the unassigned stretches (amide protons) being Gly36-Gln53, Asn57, Val58, Trp59, Gly69, Asn103-Leu111, Lys125, Met126, Ala165, Asn166, Asn176-Gly178, Gly186, Gly207, Lys216-Leu221, Iso246, Val247, Ala257, Leu269, and Arg270. For the C_α and C_β carbon resonances, I improved the assignment from 85% to 91% as compared to Yao's report. Furthermore, the main chain's carbonyl assignment was not reported by Yao. et.al.[80]

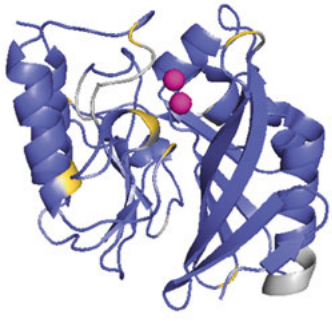

GQQMETGDQRFGDLVFRQLAPNV
WQHTSYLDMPGFGAVASNGLIVR
DGGRVLVVDTAWTDDQTAQILNW
IKQEINLPVALAVVTHAHQDKMGG
MDALHAAGIATYANALSNQLAPQE
GMVAAQHSLTFAANGWVEPATAP
NFGPLKVFYPGPGHTSDNITVGIDG
TDIAFGGCLIKDSKAKSLGNLGDAD
TEHYAASARAFGAAFPKASMIVMS
HSAPDSRAAITHTARMADKLR

Figure 30. The NMR main-chain assignment of NDM-1 (The PDB:5XP6[83] crystal structure was used for visualization): yellow – ^{1}H and ^{15}N not assigned; only Cα and Cβ (if existing) assigned; blue – ^{1}H, ^{15}N, Cα and Cβ assigned (if existing); black– not assigned; underlined– active center, or amino acid expected to interact with inhibitors.

GQQMETGDQRFGDLVFRQLAPNV
WQHTSYLDMPGFGAVASNGLIVR
DGGRVLVVDTAWTDDQTAQILNW
IKQEINLPVALAVVTHAHQDKMGG
MDALHAAGIATYANALSNQLAPQE
GMVAAQHSLTFAANGWVEPATAP
NFGPLKVFYPGPGHTSDNITVGIDG
TDIAFGGCLIKDSKAKSLGNLGDAD
TEHYAASARAFGAAFPKASMIVMS
HSAPDSRAAITHTARMADKLR

Figure 31. The NMR main-chain assignment of NDM-1 (The PDB:5XP6[83] crystal structure was used for visualization): green– assigned CO; black– not assigned; underlined– active center, or amino acid expected to interact with inhibitors.

5.3. NMR spectroscopic determination of the binding site of the inhibitors

Nuclear magnetic resonance (NMR) spectroscopy and X-ray crystallography are the standard techniques for the assessment of protein-ligand binding. Whereas NMR spectra are time-averaged on the time-scale of nanoseconds to seconds, X-ray diffraction data is time-averaged over seconds to hours. Whereas X-ray studies primarily provide ‘static’ three-dimensional depictions

of rigidified (crystallized) molecular structures, solution NMR spectra provides information about both structure and dynamics, under close to physiological conditions.[84] NMR is, however, limited in terms of molecule size.

In this thesis, I chose to study protein-inhibitor binding events with target-based NMR approaches. For all three series of the compounds (Chapter 4) inhibitor binding induced chemical shift perturbation experiments were performed. Out of the phosphonamidates described in Chapter 4.1 (Paper I), compound **19d** was selected for NMR studies, motivated by its high aqueous solubility. We monitored $^{1}H,^{15}N$ chemical changes ($\Delta\delta$) upon addition of small aliquots of the inhibitor for each amino acid of ^{15}N-labelled NDM-1 (assignment Chapter 5.2). The chemical shift changes were then visualized in a histogram as a function of the amino acid position in the protein. Throughout the titration, a single set of signals were observed, which indicates a rapid association-dissociation process as compared to the NMR timescale. As the chemical shift depends on the environment, the observed chemical shift is the population average of the free and the bound forms. The chemical shift changes as a function of the inhibitor concentration detected on a selected amino acid within the binding cleft may provide a binding curve that allows determination of the binding strength, whereas analysis of the chemical shift changes observed at different amino acids at a certain inhibitor concentration may allow pinpointing the protein residues that are involved in the protein-inhibitor interaction. Chemical shift changes can be caused directly by binding, or indirectly by binding induced conformational change.

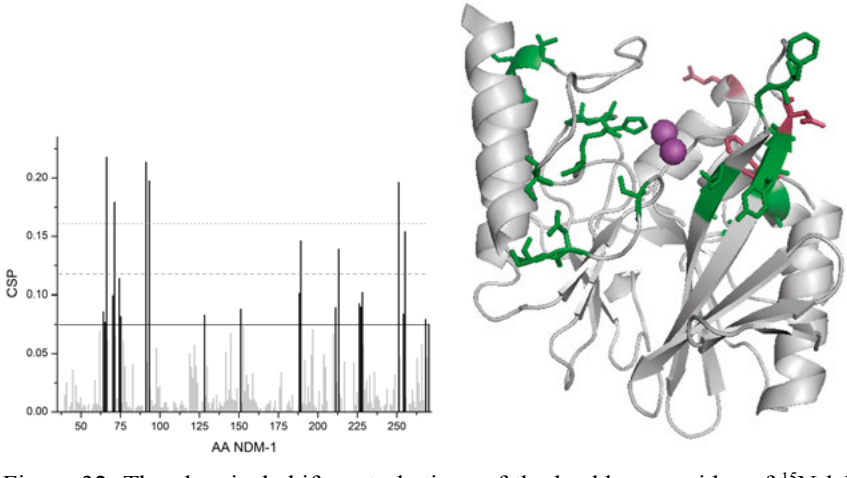

Figure 32. The chemical shift perturbations of the backbone amides of ^{15}N-labelled NDM-1 upon addition of **19d**. Bars with a height greater than the population mean plus one standard deviation ($\mu+1\sigma$ - solid line; black bars) indicate the residues significantly influenced by ligand binding (left). NDM-1 structure with highlighted significant CSP (green) and NOE detected resonances (pink) was presented above (right).

The binding induced chemical shift changes were visualized as a function of amino acid position (Figure 32), and population mean plus one standard deviation ($\mu+1\sigma$) was considered as significant.[60] The residues Asp66, Gly71, Trp93, and Ser251 were showing the largest CSPs (with ligand concentration of 2.37 mM), larger than the population mean plus three standard deviations ($\mu+3\sigma$). These amino acids have been reported to interact with NDM-1 inhibitors previously.[85] ASL1, L5, and ASL5 contained amino acids with significant CSPs. Large chemical shift changes in a specific region of the protein, whereas no significant changes in other parts indicates specific binding (see a more detailed description in Paper I in the section *NMR characterization of phosphonamidate binding*). The binding site identified with chemical shift perturbation experiments (pink-colored residues in Figure 20) were further confirmed by intermolecular NOEs detected by 3D ^{15}N-filtered HSQC-NOESY (Expansion can be found In Paper I Figure 7).

Out of the α-aminophosphonic acid inhibitors (Chapter 4.2), eleven compounds showing activity against NDM-1, and twenty against VIM-2 were selected for NMR investigation. For comparativity, the protein concentration was kept at 250 μM and a 7-step titration was performed adding 0, 0.5, 1, 2, 4, 8, and 16 equivalents of inhibitor. High concentration stock solutions of the ligands were prepared (0.5 equivalents of ligand in 1 μL of buffer), as this gives most reliable results not inducing significant chemical shift changes upon dilution. CSP histograms are presented in the *Supporting Information* of Paper II. The superimposed chemical shift changes from 5 (**26b-1**, **26c-1**, **26i-1/2** and **26j-1**) and 7 (**26a-1**, **26b-1/2**, **26c-1/2**, **26i-2**, and **26j-1)** titrations of NDM-1 and VIM-2, respectively, are shown in Figure 33, and Figure 34. For NDM-1, a single set of population averaged signals were observed, indicative of the ligand inhibitor binding being a process faster than the NMR timescale. For VIM-2 the broadening and reappearing of some initially broadened signals was observed during the titration, suggesting the binding to be in the fast to intermediate exchange regime.

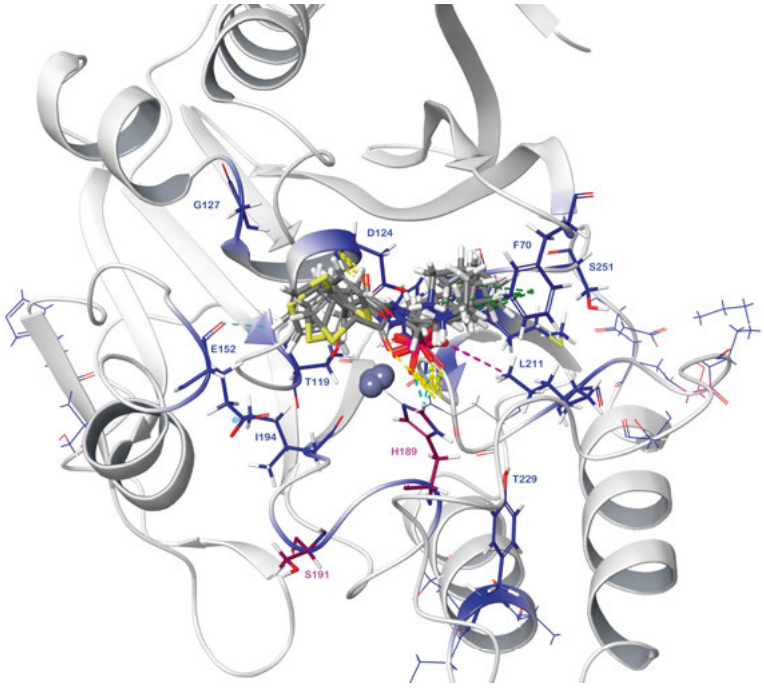

Figure 33. The chemical shift perturbation of the backbone amides (CSP) of ^{15}N-labelled NDM-1 upon titration of α-aminophosphonic acid inhibitors (Table 2). Residues with CSP greater than the population mean plus one standard deviation (μ+1σ) are considered to be significantly influenced by ligand binding. Surfaces colored dark blue colors were affected consistently, purple the majority of the time, and light blue was inconsistent, between the ligands.

A significant number of resonances were affected upon titration with inhibitors. Amino acids Phe70, Asp124, and Lys211 of NDM-1 were pinpointed to be part of the active site (Figure 33) as these were affected in titrations with every ligand. Significant chemical shift perturbations were found[85] for Tyr 65, Tyr199, Arg203, Ser205, and His238 of VIM-2 (Figure 34) throughout titrations with every inhibitor (details are given in the *Supporting Information* of Paper II).

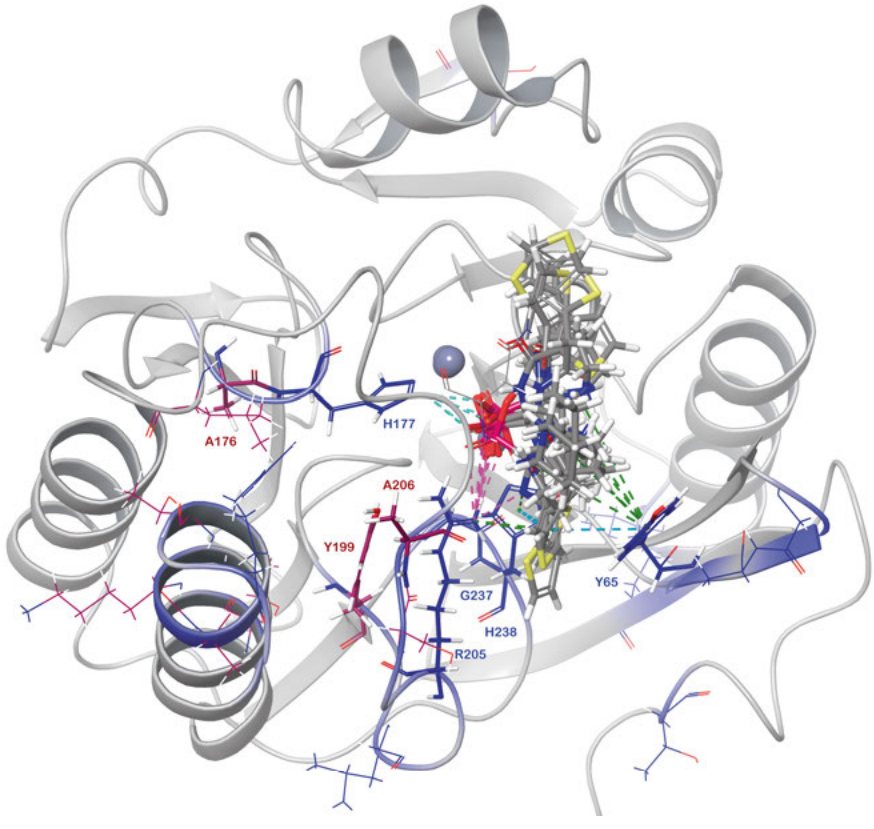

Figure 34. The chemical shift perturbation of the backbone amides (CSP) of ^{15}N-labelled NDM-1 upon titration of α-aminophosphonic acid inhibitors (Table 2). Residues with CSP greater than the population mean plus one standard deviation (μ+1σ) are considered to be significantly influenced by ligand binding. Surfaces coloured dark blue colours were affected consistently, purple the majority of the time, and light blue was inconsistent, between the ligands.

In order to determine whether the structurally closely related inhibitors possess the same binding site and binding mode, the chemical shift changes observed upon addition of inhibitors **26b-1**, **26c-1**, **26i-2** and **26j-1**, for NDM-1 and **26a-1**, **26b-1/2**, **26c-2**, **26i-2**, and **26j-1**, for VIM-2 were correlated to that observed for inhibitor **26i-1**. (Figure 35) The linear correlation of the chemical shift changes indicated that the inhibitors adopt a similar binding mode in the same binding site. The R^2 values of NDM-1 for all inhibitors were in the range of 0.81–0.84, and most of the affected resonances were found to be consistent. For VIM-2, the R^2 values were in the range of 0.61–0.82. For this enzyme, a larger number of CSPs were found to be substrate specific.

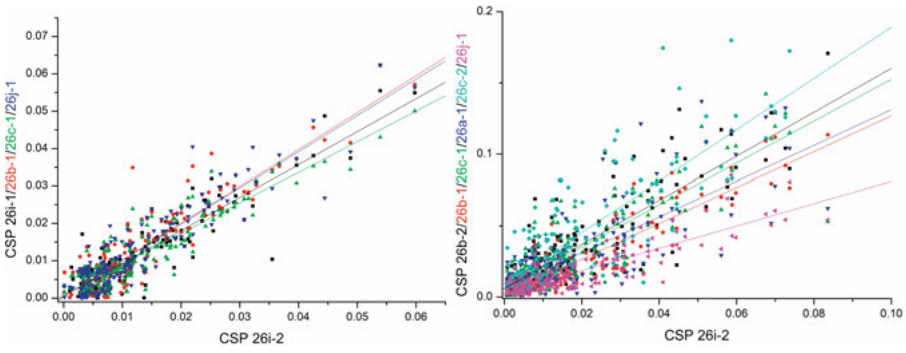

Figure 35. The correlation of the chemical shift perturbations observed for NDM-1 (left) and VIM-2 (right) upon titration with inhibitors, as a function of the chemical shift changes observed upon titration with **26i-2**.

The dissociation constants (K_d) of the complexes of titrated α-aminophosphonic acid inhibitors with NDM-1 and VIM-2 (Chapter 4.2) were estimated, based on the observed concentration dependent chemical shift changes, using equation *2* (Chapter 3.3), with the results being given in Table 2.

Table 2. The dissociation constants (K_d) estimated for the complexes of titrated α-aminophosphonic acid inhibitors with NDM-1 and VIM-2 based on the concentration dependent chemical shift perturbations.

Protein / Compound	NDM-1 [mM]	VIM-2 [mM]
26b-1	1.98 +/- 0.14	0.92 +/- 0.09
26b-2	n.d.[1]	0.38 +/- 0.04
26c-1	3.10 +/- 0.32	1.40 +/- 0.05
26c-2	n.d.	0.44 +/- 0.03
26i-1	0.52 +/- 0.04	n.d.
26i-2	1.39 +/- 0.13	1.46 +/- 0.19
26j-1	2.20 +/- 0.19	1.11 +/- 0.11

[1] n.d. = not detected

The titration of fluorine-labelled ligands (Chapter 4.3) allowed the investigations of their binding using ^{19}F NMR detection. This avoids signal overlaps, not unusual with ^{1}H,^{15}N HOSQC detection. The advantages of ^{19}F NMR can be either used by fluorine-labelling of proteins, as was presented by E. van Groesen et.al.,[86] or upon using ligands that contain fluorine. In this work, the second approach was applied. Chemical shift perturbation experiments (^{1}H,^{15}N HSQC) were carried out for both **28-1** and **28-2** enantiomers of the fluorinated inhibitor (Figure 36). Throughout the titration, protein signals be-

longing to both the free and the bound inhibitor were observed, which indicates that the protein binding is a slow process as compared to the NMR timescale.

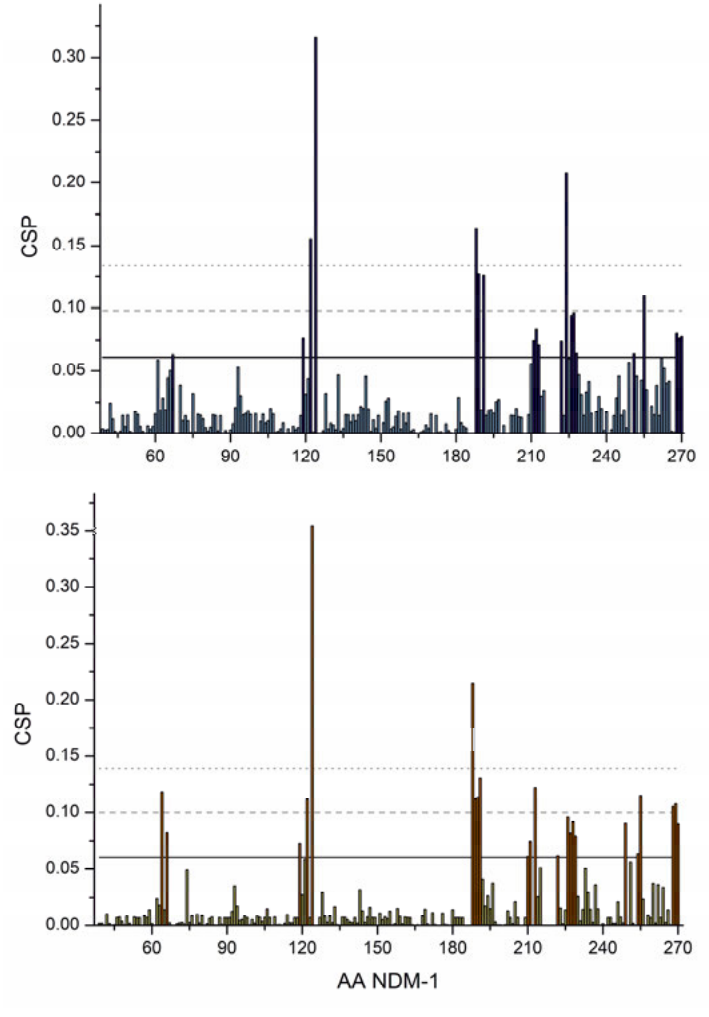

Figure 36. The chemical shift perturbations observed for the backbone amides of ^{15}N-labelled NDM-1 upon addition of **28-1** and **28-2**. Bars with a height greater than the population mean plus one standard deviation ($\mu+1\sigma$ - solid line; navy (top) and orange (bottom)) indicate the residues (named in paragraph below) significantly influenced by ligand binding.

Stereoisomer **28-1** was observed to possess higher activity **28-2**. It also showed higher solubility (buffer with 2.5% of DMSO), and therefore the CSP analyses were performed using up to 15 and 10 equivalents of **28-1** and **28-2**,

respectively. The binding induced chemical shift changes were most significant on Thr119, His122, Asp124, Gly188, His189, Ser191, Lys211, Asp212, Ser21S, Gly222, Thr226, Glu227, His228, Ser255, Lys268, Leu269, and Arg270. The dissociation constant of the **28-1** – NDM-1 complex was estimated to 149.2 μM, by fitting the signal intensity of the bound species to equation *3* (Chapter 3.3). Details of the analysis are given in Paper III. Due to the limited solubility of **28-2**, its K_d could not be reliably calculated.

The $^{19}F,^{1}H$ HOESY studies performed for the complex of **28-1** and NDM-1 HOE correlations indicated Met67, His122 and Trp93 to be in close proximity of the CF_3-group of the inhibitor.

5.4. Molecular docking studies

To gain further insight into the binding mode of the inhibitors, we performed computational dockings selecting the most probable binding modes based on NMR data and predicted binding energies. For all compounds, protein crystal structures with a resolution of <2Å were applied as starting points, and flexible docking followed by MM-GBSA rescoring calculations were used with Glide, followed by Prime, as implemented in the software package Schrödinger.

The proposed binding pose for phosphonamide **19d** was selected based on the CSP data and protein-inhibitor intermolecular NOE signals (Figure 37). The amino acids Phe70, Trp93, and Asn220 of NDM-1were observed to take part in inhibitor binding. These residues also showed large binding-induced CSPs (Chapter 5.3). The hypothesis that these amino acids play a key role in binding is in agreement with the literature.[85] Based on the significant CSP of His189, Zn2 interacts with the phosphonamidate inhibitors, but not Zn1. The binding of **19d** is suggested to be mediated by edge-to-face π–π interactions of the hydrophobic and flexible pyridine moieties with Phe70 and Trp93.

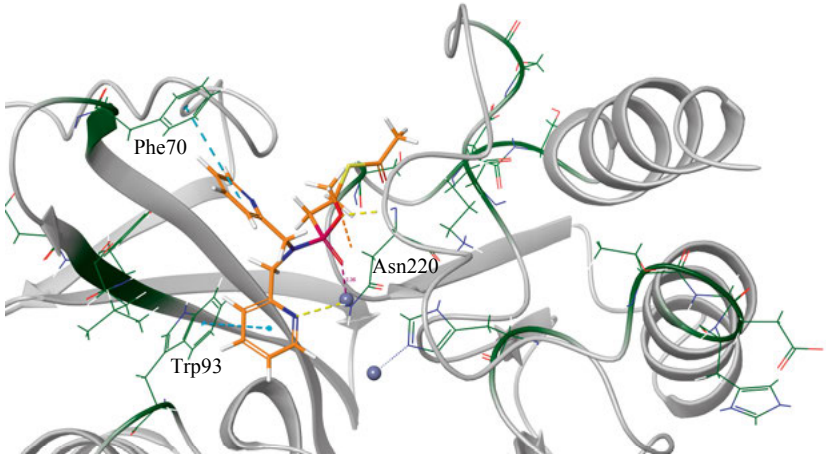

Figure 37. The interactions of **19d** with NDM-1, as identified by molecular docking, and selected based on NMR evidences.

For all α-aminophosphonic acid inhibitors that were studied using NMR titration, molecular docking was performed starting from the X-ray structures PDB:6O5T[87]and PDB:603R[87]. Herein, the analysis of the docking studies performed for **26c-1** in complex with NDM-1 and VIM-2 are presented (Figure 38) whereas all data is given as Supporting Information of Paper II. Strong trend of two binding modes was observed, in which Phe70 / Tyr 67 were detected to contribute in π-cation interaction with the piperidine moiety, or in a face-to-edge π–π stacking with its thiophene ring. The first was proposed to be more probable. The binding poses ranked highest for both NDM-1 and VIM-2 had comparable binding energies: ΔG(NDM-1) -44.62 kcal/mol and ΔG(VIM-2) -48.50 kcal/mol. Cation-π interactions of the phosphonic acid moiety with Phe70 (NDM-1) / Tyr65 (VIM-2) and with one of the zinc ions was suggested to be one of the forces stabilizing the complex. For both complexes, hydrogen bonds to Asn220 (NDM-1) /Asn208 (VIM-2) and Asp124 (NDM-1) / Asp116 (VIM-2) were observed, and T-shaped π–π interactions with Phe70 (NDM-1) / Tyr65 (VIM-2). Detailed docking results were discussed in the Paper II in section *Computational Docking.*

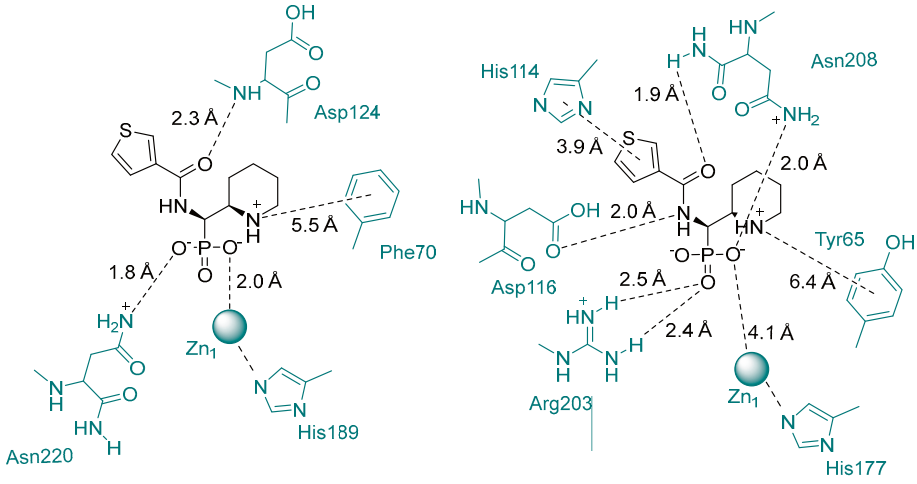

Figure 38. Representation of the protein-inhibitor interactions for **26c-1** in complex with NDM-1 (left) and VIM-2 (right), based on molecular docking.

The docking of compounds **28** and **1** to NDM-1 was performed starting from the X-ray structure PDB:5ZIO[88]. These compounds differ in CF_3 to CH_3 substitution (Figure 39).

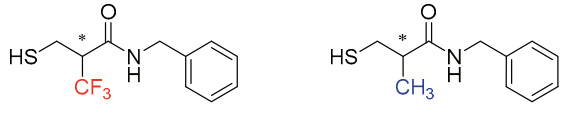

28 **1**

Figure 39. The compounds belonging to Series 3 which were used in the molecular docking studies.

Enantiomer *S* for **28** and enantiomer *R* for **1** were predicted to bind the strongest to NDM-1, with comparable orientation in the binding site (Figure 27). This hypothesis should be confirmed by X-ray diffraction. The computed binding modes (docking) and the bind energies (ΔG) were comparable for these compounds, namely ΔG_{bind} **28**(*S*) = -58.7 kcal/mol and ΔG_{bind} **1**(*R*) = -58. 5 kcal/mol, respectively. The amino acids Met67, Trp93, His122, Gln123, Asp124 and Asn220 were within 5 Å from the $-CF_3$ / $-CH_3$ functionalities. Out of these, intermolecular HOESY cross-peaks were observed for Met67, His122 and Trp93. This may indicate that the $-CF_3$ group of **27** is oriented towards loop3 in its NDM-1 complex.

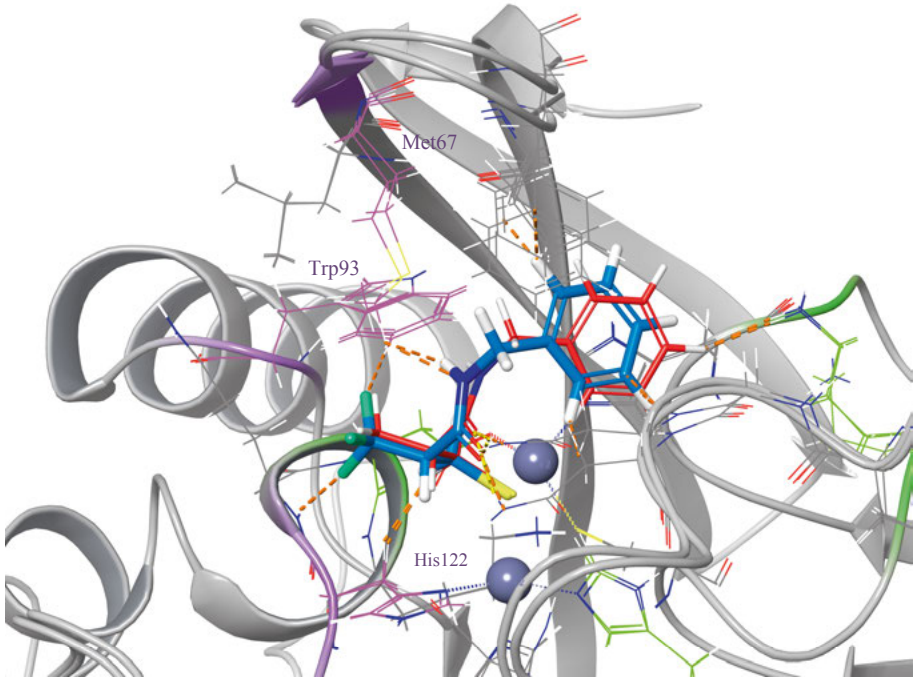

Figure 40. Superimposed complexes of **28** and **1** in complex with NDM-1, as proposed by molecular docking. The key interactions, and the experimentally observed HOESY correlations are highlighted in purple, and significant CSPs in green.

In the proposed binding mode, both zinc ions coordinate to the sulfur of the inhibitor (Figure 40). Additionally, the -CF_3 group forms an N–H···F–C hydrogen bond with the side chain amine of Gln123. This could, however, not be confirmed by NMR, neither by CSPs or HOESY correlations and therefore should be considered with scepticism. Although it is important to take into consideration that docking is dependent from crystalized form which might not be the lowest energy state,[89] therefore the optimal ranges of geometric parameters are taken into account during docking.[90]

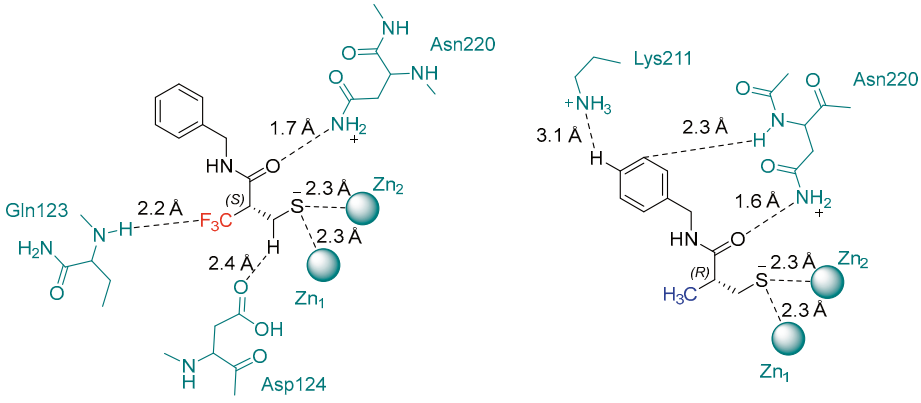

Figure 41. The protein-ligand interactions for **28** and **1** with NDM-1, proposed based on computational docking.

6. Concluding remarks and perspective

This thesis described the development of metallo-β-lactamase inhibitors and the investigation of their binding to metallo-β-lactamases. Based on the NMR spectroscopic studies and computational docking of three groups of inhibitors, the following knowledge was gained:

- The NMR backbone resonance assignment of NDM-1 was established. This provides basis for future solution NMR-based studies of the protein–inhibitor complex, supporting the development of future metallo-β-lactamase inhibitors.

- A phosponamidate moiety was used to mimic the tetrahedral transition state of β-lactam hydrolysis. A series of potential inhibitors were designed, synthesized and evaluated. Five compounds showed inhibitory activity against NDM-1, VIM-2 or GIM-1 in enzyme inhibition assays. The most potent inhibitory activity, IC_{50} of 86 μM was observed against GIM-1. Compound **19b**, which showed activity against NDM-1, was used for solution NMR and computational docking based identification of its binding site and binding mode to NDM-1.

- α-Aminophosphonic acids were successfully identified as potential metallo-β-lactamase inhibitors. Some of them showed good inhibitory activity (< 100 μM) against VIM-2. Their binding modes to VIM-2 and NDM-1 were compared. This comparative study is expected to provide useful information for future wide-spectrum inhibitors.

- Despite the limiting solubility of some compounds, NMR studies allowed significant information about the binding site to be obtained.

- Chemical shift perturbation studies showed that the phosphonamidates, α-aminophosphonic acid-type inhibitors complex only one of the two zinc ions, whereas fluorine-labelled ligands coordi-

nates both zinc ions. The coordination is by an oxygen of the phosphonic acid/ester moiety, or by sulfur of the thiol moiety, respectively.

- Inhibitor induced chemical shift perturbation studies indicated that the binding of α-aminophosphonic acid inhibitors has different time scale for NDM-1 and VIM-2. The inhibitors are in (Chapter 4.1 and Chapter 4.2) fast exchange between the free and NDM-1-bound form, and thus the binding induces chemical shift changes of sharp NMR signals. The VIM-2 binding of α-aminophosphonic acid-type inhibitors induced chemical shift changes of some, and broadening of other amino acid signals. Some signals broadened in the free form reappeared. This indicates that the binding is in the fast to intermediate time-scale, and that the conformational dynamics of some loops of VIM-2 are influenced by the inhibitor binding, whereas this is not observed for NDM-1.

- A trifluoromethyl-substituted analogue of a literature known inhibitor was studied using NMR and computational docking. The binding mode of this compound was found to be similar to that of its literature analogue (CH_3-functionalized), for which the binding mode was previously unidentified. This ligand coordinates to both of the zinc ions through its thiol functionality, and its association-dissociation equilibrium is slow on the NMR time scale, resulting in separate signals of the free and bound forms.

- The binding site recognition for all potential inhibitors are expected to be valuable information for design and development of broad spectrum metallo-β-lactamase inhibitors.

7. Sammanfattning på Svenska

1929-talets upptäckt av penicillin förebådade antibiotikaerans början och resulterade i en minskning av mänsklig dödlighet orsakad av enkla bakterieinfektioner. Popularisering och kraftig överanvändning av antibiotika resulterade i det världsomspännande största problemet med utveckling av bakterieresistens. Utan någon åtgärd närmar vi oss snart en punkt då enkla infektioner, såsom lunginflammation eller septikemi, kommer att ha en mycket sannolik dödlig prognos. Den mest utbredda mekanismen för bakteriell resistens är nedbrytning eller modifiering av antibiotika, innan de når målstället, av ett β-laktamas som NDM-1, VIM-2 och GIM-1, en specifik grupp av försvarsenzymer, som tillhör till samma grupp (Figur 1).

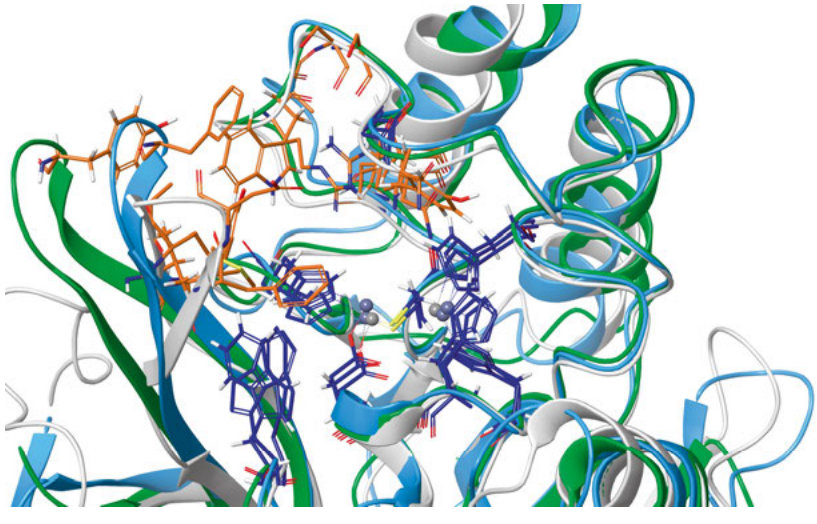

Figur 1. Överlagrade bindningsställen för NDM-1 (cyan), GIM-1 (grön) och VIM-2 (grå), där identiska AA:er visas i blått och olika AA:er visas i orange.

Den presenterade avhandlingen beskriver undersökningen av bindningsstället för metallo-β-laktamaser (MBL) med hjälp av tre olika typer av föreningar med flera tekniker. En kombination av strukturbaserad läkemedelsdesign, organisk syntes, biologisk utvärdering, nukleär magnetisk resonans (NMR) spektroskopi och molekylär dockning har använts för att rationalisera och bestämma nya MBL inhibitorer, och dessutom deras bindningssätt. Tre nya typer av inhibitorer studerades.

Den presenterade avhandlingen är indelad i sex kapitel. Det första kapitlet innehåller formulerade mål för detta arbete. I det andra kapitlet presenterar författaren den allmänna bakgrunden till bakteriell resistens, tillsammans med en beskrivning av hydrolysmekanismen, den strukturella grunden för metallo-β-laktamaser och kända inhibitorer. På grund av den tvärvetenskapliga forskningen tillägnade författaren det tredje kapitlet att kortfattat förklara alla metoder som nämns i denna avhandling: enzymanalys, assignering av proteinryggrad, perturbation av kemiska skift, NOESY-baserade experiment och molekylära dockningsstudier. Det tredje kapitlet fokuserar på de tre grupperna av studerade inhibitorer. Avsnittet om de fosfoamidatbaserade metallo-β-laktamaserna innehåller design och syntetisk beskrivning. För de fosfonsyrabaserade och fluormärkta inhibitorerna förklarar författaren syftet med de studerade föreningarna. Följande kapitel fokuserar på bindningsstudier. En kombination av de experimentella metoderna med NMR-spektroskopi används tillsammans med molekylära dockningsstudier för att bestämma bindningsstället för alla studiehämmare. Sammanfattningsvis konfirmerade denna avhandling bindningssätt för alla studerade inhibitorer, dessutom jämförde författaren två enzymer från New Delhi metallo-β-laktamas och Verona integronkodad metallo-β-laktamas och likheter fastslogs. För de fluormärkta inhibitorerna konfirmerade författaren bindningssättet för den studerade föreningen och för dess metylerade version, vilket inte tidigare har fastställts i litteraturen.

Utförda NMR-studier ledde till förbättrad assignering av New Dehli Metallo-β-laktamaser-1 (NDM-1) och resulterade framgångsrikt i förslag till bindningsställen för alla studerade inhibitorer. Ytterligare molekylära dockningsstudier med stöd av NMR-resultat gav tillförlitliga bindningspositioner. Med hjälp av denna information kan rationell utformning av metallo-b-laktamsshämmare utföras. Dessutom konfirmerades fosforhaltiga strukturer, en uppsättning piperidinserier och fosfonamidater vara bra utgångspunkter för utvecklingen av de adaptiva bredspektrumhämmarna, med potential att vara aktiva mot flera MBL.

8. Acknowledgements

> "You know how it is. You pick up a book, flip to the dedication, and find that, once again, the author has dedicated a book to someone else and not to you. "
>
> Neil Gaiman

With that said, I truly hope to acknowledge each and all of you. It has been an amazing opportunity to pursue my PhD journey in this unique place. Over the last five years, I have met a countless number of people without whom those years would not be the same. I would like to take this opportunity to express my gratitude to all of you who were part of this journey:

My mentor and supervisor *Prof Máté Erdélyi.* I am deeply grateful for the opportunity which you gave me, starting from the incredibly enjoyable interview. Over the last five years, I learned more than I have expected, scientifically, but also in a personal manner. I am truly grateful for always opening the office door to answer even the smallest questions, and for your unnumbered support, patience and encouragement. Thank you for passing your NMR passion and knowledge, but also for being a great bike companion, and neighbour!

My co-supervisor *Dr Hanna Andersson*, for being the kindest and warmest person who I have had a chance to meet in Sweden. I cannot express how much I am grateful for your care of me when I arrived, and for every discussion, help and advice I received from you. For my Road Runner character, I could not be more thankful your patience and calmness whenever I was coming with my 'waterfall of words'. It has been truly a pleasure to work with you.

Prof Annette Bayer, thank you for giving me a chance to visit your group and for the opportunity to work with Sasha on the project which became a part of this thesis. It was a really enjoyable time at UiT.

I would like to express my gratitude to *Fritz Deufel,* for your major contribution to the Piperidine series project, which allowed me to proceed with the most enjoyable protein NMR studies. You are truly precious and I am sure that you will achieve great things in life!

I would like to express my gratitude to *Adolf, Christine, Helena, Jan, and Luke* for your constant support for all of us PhD students. Also additional thanks to *Gunnar, Farshid, Johanna, Hanna, and the rest of the administrative staff*, you keep this wheel turning.

In such a multidisciplinary project, I could not do it all by myself, therefore I would like to thank you all, thanks to whom this project had a chance to progress: *Lisa Allander, Anna Andersson Rasmussen, Ulrika Brath, Angela Gronenborn, Madlen Hubert, Wolfgang Knecht, Alexandra Kondratieva, Linus Sandegren, Paula Di Santo, Hanna-Kirsti Schroder Leiros, Susann Skagseth, Per Sunnerhagen, Zoltán Takács, and Arto Valkonen,* for your collaboration and all helpful discussions!.

To all past and current members of the halogen bonding, and colleagues from outside of the group for creating a pleasant working environment: *Alan, Bea, Daniel, Duy, Emanuel, Fredrik, Hermina, Kinga, Matt, Mauricio, Merve, Scott, Sofia, Stefan, Susanne, Rui, Thobias, Yoseph (and many others)*. I would like to express my additional gratitude to Bachelor students: *Erik, Tor*, and *Loes,* for your contribution to the project. Additionally, to Master student: *Jan Luca,* despite the great work you have done, you brought a fantastic atmosphere and 'weird' music to the lab. It was fun to work with you! *Ivan* – your kindness and optimism will be truly missed, and become irreplaceable. *Lotta* and *Daniel* – for all useful advice and great after-work trips and games company! *Caroline* – thank you for answering all my biochemistry-related questions, and letting me hug you every time! *Sofia*: thank you for your correction of *Sammanfatting på Svenska*. *Rui*: thank you for proofreading this thesis!

I could not call Uppsala my home without people who were my little family, away from home: *Caro, Emma, Marta, Valter, Dragos, Ginho, Jana, and Jimmy* you are the most amazing friends which one could ask for. Thank you for all our small and big trips, for all burgers, and for all the climbing days! I am gonna miss you all. Also, *Alfred, Bea, Camille, Rianne, Rai, Venu, Hanna, Nicolo, Öyvind, Juliana, Axel, Sophie, Taylor, Adam, Maciej, Ania, and Mantas* you all made time here truly precious, and you are a part of the reason why I called Sweden 'my home' for last five years. Referring to home, I could not do it without *my parents and my family* for your unconditional support! Without my dearest friends back in Poland *Magda, Swirek, Ucho, Boba, Daniel*, and also those who significantly influence my education and career, *Marcin, Szymon, and Olexandr*!

Lastly, to my beloved life partner, *Jakub*, for your unwavering support, for constantly appreciating the smallest achievements, for putting a smile on my face, pushing me out of my comfort zone every day, and for moving for me to Sweden and sharing all moments here with me. You are inspiring me every day and I am looking forward to starting an adventure with you in our new home with a third dimension, full of Schwarznasenschafe!

This research was funded by The Swedish Research Council.

9. References

1. Fleming, A., On the Antibacterial Action of Cultures of a Penicillium, with Special Reference to their Use in the Isolation of B. influenzæ. *Br. J. Exp. Pathol.* **1929,** *10* (3), 226-236.
2. Quinn, R., Rethinking antibiotic research and development: World War II and the penicillin collaborative. *Am. J. Public. Health.* **2013,** *103* (3), 426-34.
3. Barber, M.; Rozwadowska-Dowzenko, M., Infection by penicillin-resistant staphylococci. *Lancet (London, England)* **1948,** *2* (6530), 641-4.
4. Hutchings, M. I.; Truman, A. W.; Wilkinson, B., Antibiotics: past, present and future. *Curr. Opin. Microbiol.* **2019,** *51*, 72-80.
5. World Health Organization, *Global action plan on antimicrobial resistance*. World Health Organization: Geneva, 2015.
6. Hamed, R. B.; Gomez-Castellanos, J. R.; Henry, L.; Ducho, C.; McDonough, M. A.; Schofield, C. J., The enzymes of β-lactam biosynthesis. *Nat. Prod. Rep.* **2013,** *30* (1), 21-107.
7. Munita, J. M.; Arias, C. A., Mechanisms of Antibiotic Resistance. *Microbiol. Spectr.* **2016,** *4* (2), 1-24.
8. World Health Organization, Antibiotic resistance: global report on surveillance. **2014**.
9. O'Neill, J., Antimicrobial Resistance: Tackling a crisis for the health and wealth of nations. *AMR Review* **2014**, 1-20.
10. Czaplewski, L.; Bax, R.; Clokie, M.; Dawson, M.; Fairhead, H.; Fischetti, V. A.; Foster, S.; Gilmore, B. F.; Hancock, R. E. W.; Harper, D.; Henderson, I. R.; Hilpert, K.; Jones, B. V.; Kadioglu, A.; Knowles, D.; Ólafsdóttir, S.; Payne, D.; Projan, S.; Shaunak, S.; Silverman, J.; Thomas, C. M.; Trust, T. J.; Warn, P.; Rex, J. H., Alternatives to antibiotics—a pipeline portfolio review. *Lancet Infect. Dis.* **2016,** *16* (2), 239-251.
11. Kumar, M.; Sarma, D. K.; Shubham, S.; Kumawat, M.; Verma, V.; Nina, P. B.; JP, D.; Kumar, S.; Singh, B.; Tiwari, R. R., Futuristic Non-antibiotic Therapies to Combat Antibiotic Resistance: A Review. *Front. Microbiol.* **2021,** *12*.
12. Silver, L. L., Challenges of antibacterial discovery. *Clin. Microbiol. Rev.* **2011,** *24* (1), 71-109.
13. Wilke, M. S.; Lovering, A. L.; Strynadka, N. C., Beta-lactam antibiotic resistance: a current structural perspective. *Curr. Opin. Microbiol.* **2005,** *8* (5), 525-33.
14. Dever, L. A.; Dermody, T. S., Mechanisms of Bacterial Resistance to Antibiotics. *Arch. Intern. Med.* **1991,** *151* (5), 886-895.
15. Kapoor, G.; Saigal, S.; Elongavan, A., Action and resistance mechanisms of antibiotics: A guide for clinicians. *J. Anaesthesiol. Clin. Pharmacol.* **2017,** *33* (3).
16. Reygaert, W. C., An overview of the antimicrobial resistance mechanisms of bacteria. *AIMS Microbiol.* **2018,** *4* (3), 482-501.

17. Munita, J. M.; Arias, C. A.; Kudva, I. T.; Zhang, Q., Mechanisms of Antibiotic Resistance. *Microbiol. Spectr.* **2016,** *4* (2), 1-24.
18. Jacobs, T. G.; Robertson, J.; van den Ham, H. A.; Iwamoto, K.; Bak Pedersen, H.; Mantel-Teeuwisse, A. K., Assessing the impact of law enforcement to reduce over-the-counter (OTC) sales of antibiotics in low- and middle-income countries; a systematic literature review. *BMC Health Serv. Res.* **2019,** *19* (1), 536.
19. Sulis, G.; Adam, P.; Nafade, V.; Gore, G.; Daniels, B.; Daftary, A.; Das, J.; Gandra, S.; Pai, M., Antibiotic prescription practices in primary care in low- and middle-income countries: A systematic review and meta-analysis. *PLOS Medicine* **2020,** *17* (6), 1-20.
20. Plackett, B., Why big pharma has abandoned antibiotics. *Nature* **2020,** *586*, 50-52.
21. Bassetti, M.; Righi, E., New antibiotics and antimicrobial combination therapy for the treatment of gram-negative bacterial infections. *Curr. Opin. Crit. Care.* **2015,** *21* (5).
22. Zarkotou, O.; Pournaras, S.; Tselioti, P.; Dragoumanos, V.; Pitiriga, V.; Ranellou, K.; Prekates, A.; Themeli-Digalaki, K.; Tsakris, A., Predictors of mortality in patients with bloodstream infections caused by KPC-producing Klebsiella pneumoniae and impact of appropriate antimicrobial treatment. *Clin. Microbiol. Infect.* **2011,** *17* (12), 1798-803.
23. Batirel, A.; Balkan, II; Karabay, O.; Agalar, C.; Akalin, S.; Alici, O.; Alp, E.; Altay, F. A.; Altin, N.; Arslan, F.; Aslan, T.; Bekiroglu, N.; Cesur, S.; Celik, A. D.; Dogan, M.; Durdu, B.; Duygu, F.; Engin, A.; Engin, D. O.; Gonen, I.; Guclu, E.; Guven, T.; Hatipoglu, C. A.; Hosoglu, S.; Karahocagil, M. K.; Kilic, A. U.; Ormen, B.; Ozdemir, D.; Ozer, S.; Oztoprak, N.; Sezak, N.; Turhan, V.; Turker, N.; Yilmaz, H., Comparison of colistin-carbapenem, colistin-sulbactam, and colistin plus other antibacterial agents for the treatment of extremely drug-resistant Acinetobacter baumannii bloodstream infections. *Eur. J. Clin. Microbiol. Infect. Dis.* **2014,** *33* (8), 1311-22.
24. Daikos, G. L.; Petrikkos, P.; Psichogiou, M.; Kosmidis, C.; Vryonis, E.; Skoutelis, A.; Georgousi, K.; Tzouvelekis, L. S.; Tassios, P. T.; Bamia, C.; Petrikkos, G., Prospective observational study of the impact of VIM-1 metallo-beta-lactamase on the outcome of patients with Klebsiella pneumoniae bloodstream infections. *Antimicrob. Agents. Chemother.* **2009,** *53* (5), 1868-73.
25. Somboro, A. M.; Amoako, D. G.; Osei Sekyere, J.; Kumalo, H. M.; Khan, R.; Bester, L. A.; Essack, S. Y., 1,4,7-Triazacyclononane Restores the Activity of β-Lactam Antibiotics against Metallo-β-Lactamase-Producing Enterobacteriaceae: Exploration of Potential Metallo-β-Lactamase Inhibitors. *Appl. Environ. Microbiol.* **2019,** *85* (3), 1-13.
26. Linciano, P.; Cendron, L.; Gianquinto, E.; Spyrakis, F.; Tondi, D., Ten Years with New Delhi Metallo-β-lactamase-1 (NDM-1): From Structural Insights to Inhibitor Design. *ACS Infect. Dis.* **2019,** *5* (1), 9-34.
27. Cala, O.; Guillière, F.; Krimm, I., NMR-based analysis of protein-ligand interactions. *Anal. Bioanal. Chem.* **2014,** *406* (4), 943-56.
28. Sugiki, T.; Furuita, K.; Fujiwara, T.; Kojima, C., Current NMR Techniques for Structure-Based Drug Discovery. *Molecules* **2018,** *23* (1).
29. Grünewald, H., *Nobel Lectures. Physiology or Medicine 1942–1962*. Elsevier Publishing Company: Amsterdam, 1964.

30. Sauvage, E.; Kerff, F.; Terrak, M.; Ayala, J. A.; Charlier, P., The penicillin-binding proteins: structure and role in peptidoglycan biosynthesis. *FEMS Microbiol. Rev.* **2008,** *32* (2), 234-258.
31. Ambler, R. P., The structure of beta-lactamases. *Philos. Trans. R. Soc. Lond., B, Biol. Sci.* **1980,** *289* (1036), 321-31.
32. Jaurin, B.; Grundström, T., ampC cephalosporinase of Escherichia coli K-12 has a different evolutionary origin from that of beta-lactamases of the penicillinase type. *Proc. Natl. Acad. Sci. U.S.A.* **1981,** *78* (8), 4897-901.
33. Ouellette, M.; Bissonnette, L.; Roy, P. H., Precise insertion of antibiotic resistance determinants into Tn21-like transposons: nucleotide sequence of the OXA-1 beta-lactamase gene. *Proc. Natl. Acad. Sci. U. S. A.* **1987,** *84* (21), 7378-82.
34. Hall, B. G.; Barlow, M., Revised Ambler classification of β-lactamases. *J. Antimicrob. Chemother.* **2005,** *55* (6), 1050-1051.
35. Palzkill, T., Metallo-β-lactamase structure and function. *Ann. N. Y. Acad. Sci.* **2013,** *1277*, 91-104.
36. Fisher, J. F.; Meroueh, S. O.; Mobashery, S., Bacterial resistance to beta-lactam antibiotics: compelling opportunism, compelling opportunity. *Chem. Rev.* **2005,** *105* (2), 395-424.
37. Drawz, S. M.; Bonomo, R. A., Three Decades of β-Lactamase Inhibitors. *Clin. Microbiol. Rev.* **2010,** *23* (1), 160-201.
38. Meini, M. R.; Llarrull, L. I.; Vila, A. J., Overcoming differences: The catalytic mechanism of metallo-β-lactamases. *FEBS Lett.* **2015,** *589* (22), 3419-32.
39. Mojica, M. F.; Bonomo, R. A.; Fast, W., B1-Metallo-β-Lactamases: Where Do We Stand? *Curr. Drug. Targets.* **2016,** *17* (9), 1029-50.
40. King, D.; Strynadka, N., Crystal structure of New Delhi metallo-β-lactamase reveals molecular basis for antibiotic resistance. *Prot. Sci.* **2011,** *20* (9), 1484-91.
41. Aitha, M.; Moller, A. J.; Sahu, I. D.; Horitani, M.; Tierney, D. L.; Crowder, M. W., Investigating the position of the hairpin loop in New Delhi metallo-β-lactamase, NDM-1, during catalysis and inhibitor binding. *J. Inorg. Biochem.* **2016,** *156*, 35-39.
42. Bush, K.; Bradford, P. A., Interplay between β-lactamases and new β-lactamase inhibitors. *Nat. Rev. Microbiol.* **2019,** *17* (5), 295-306.
43. Montagner, C.; Nigen, M.; Jacquin, O.; Willet, N.; Dumoulin, M.; Karsisiotis, A. I.; Roberts, G. C. K.; Damblon, C.; Redfield, C.; Matagne, A., The Role of Active Site Flexible Loops in Catalysis and of Zinc in Conformational Stability of Bacillus cereus 569/H/9 β-Lactamase. *J. Biol. Chem.* **2016,** *291* (31), 16124-16137.
44. Linciano, P., Cendron, L., Gianquinto, E., Spyrakis, F., Tondi, D., Ten Years with New Delhi Metallo-β-lactamase-1 (NDM-1): From Structural Insights to Inhibitor Design. *ACS Infect. Dis.* **2019,** *5* (1), 9-34.
45. Yusof, Y., Tan, D. T. C., Arjomandi, O. K., Schenk, G., McGeary, R. P., Captopril analogues as metallo-β-lactamase inhibitors. *Bioorg. Med. Chem. Lett.* **2016,** *26* (6), 1589-1593.
46. King, D. T.; Worrall, L. J.; Gruninger, R.; Strynadka, N. C. J., New Delhi Metallo-β-Lactamase: Structural Insights into β-Lactam Recognition and Inhibition. *J. Am. Chem. Soc.* **2012,** *134* (28), 11362-11365.
47. Li, N., Xu, Y., Xia, Q., Bai, C., Wang, T., Wang, L., He, D., Xie, N., Li, L., Wang, J., Zhou, H. G., Xu, F., Yang, C., Zhang, Q., Yin, Z., Guo, Y., Chen, Y., Simplified captopril analogues as NDM-1 inhibitors. *Bioorg. Med. Chem. Lett.* **2014,** *24* (1), 386-389.

48. Liu, S., Jing, L., Yu, Z. J., Wu, C., Zheng, Y., Zhang, E., Chen, Q., Yu, Y., Guo, L., Wu, Y., Li, G. B., ((S)-3-Mercapto-2-methylpropanamido)acetic acid derivatives as metallo-β-lactamase inhibitors: Synthesis, kinetic and crystallographic studies. *Eur. J. Med. Chem.* **2018,** *145*, 649-660.
49. Büttner, D., Kramer, J. S., Klingler, F. M., Wittmann, S. K., Hartmann, M. R., Kurz, C. G., Kohnhäuser, D., Weizel, L., Brüggerhoff, A., Frank, D., Steinhilber, D., Wichelhaus, T. A., Pogoryelov, D., Proschak, E., Challenges in the Development of a Thiol-Based Broad-Spectrum Inhibitor for Metallo-β-Lactamases. *ACS Infect. Dis.* **2018,** *4* (3), 360-372.
50. Ma, J., Cao, Q., McLeod, S. M., Ferguson, K., Gao, N., Breeze, A. L., Hu, J., Target-based whole-cell screening by (1)H NMR spectroscopy. *Angew. Chem. Int. Ed. Engl.* **2015,** *54* (16), 4764-7.
51. Cain, R., Brem, J., Zollman, D., McDonough, M. A., Johnson, R. M., Spencer, J., Makena, A., Abboud, M. I., Cahill, S., Lee, S. Y., McHugh, P. J., Schofield, C. J., Fishwick, C. W. G., In Silico Fragment-Based Design Identifies Subfamily B1 Metallo-β-lactamase Inhibitors. *J. Med. Chem.* **2018,** *61* (3), 1255-1260.
52. Skagseth, S., Akhter, S., Paulsen, M. H., Muhammad, Z., Lauksund, S., Samuelsen, O., Leiros, H. S., Bayer, A., Metallo-β-lactamase inhibitors by bioisosteric replacement: Preparation, activity and binding. *Eur. J. Med. Chem.* **2017,** *135*, 159-173.
53. Christopeit, T.; Leiros, H.-K. S., Fragment-based discovery of inhibitor scaffolds targeting the metallo-β-lactamases NDM-1 and VIM-2. *Bioorg. Med. Chem. Lett.* **2016,** *26* (8), 1973-1977.
54. Yung-Chi, C.; Prusoff, W. H., Relationship between the inhibition constant (KI) and the concentration of inhibitor which causes 50 per cent inhibition (I50) of an enzymatic reaction. *Biochem. Pharmacol.* **1973,** *22* (23), 3099-3108.
55. Grzesiek, S.; Bax, A., Improved 3D triple-resonance NMR techniques applied to a 31 kDa protein. *J. Mag. Reson.* **1992,** *96* (2), 432-440.
56. Wittekind, M.; Mueller, L., HNCACB, a High-Sensitivity 3D NMR Experiment to Correlate Amide-Proton and Nitrogen Resonances with the Alpha- and Beta-Carbon Resonances in Proteins. *J. Magn. Reson.* **1993,** *101* (2), 201-205.
57. Yamazaki, T.; Lee, W.; Arrowsmith, C. H.; Muhandiram, D. R.; Kay, L. E., A Suite of Triple Resonance NMR Experiments for the Backbone Assignment of 15N, 13C, 2H Labeled Proteins with High Sensitivity. *J. Am. Chem. Soc.* **1994,** *116* (26), 11655-11666.
58. Clubb, R. T.; Thanabal, V.; Wagner, G., A constant-time three-dimensional triple-resonance pulse scheme to correlate intraresidue 1HN, 15N, and 13C′ chemical shifts in 15N-13C-labelled proteins. *J. Magn. Reson.* **1992,** *97* (1), 213-217.
59. Kovacs, H., Introduction to 3-dimensional and triple resonance NMR-spectroscopy with focus on biomolecules on Avance spectrometers. *Bruker AG* **2003**, 1-89.
60. Williamson, M. P., Using chemical shift perturbation to characterise ligand binding. *Prog. Nucl. Magn. Reson. Spectrosc.* **2013,** *73*, 1-16.
61. Fielding, L., NMR methods for the determination of protein-ligand dissociation constants. *Curr. Top. Med. Chem.* **2003,** *3* (1), 39-53.
62. Gronenborn, G. M. C. a. A. M., Theory of the Time Dependent Transferred Nuclear Overhauser Effect: Applications to Structural Analysis of Ligand-Protein Complexes in Solution. *J. Mag. Reson.* **1983,** *53*, 423-442.

63. Becker, W.; Bhattiprolu, K. C.; Gubensäk, N.; Zangger, K., Investigating Protein-Ligand Interactions by Solution Nuclear Magnetic Resonance Spectroscopy. *ChemPhysChem.* **2018,** *19* (8), 895-906.
64. David Neuhaus, M. R. W., *The nuclear overhauser effect in structural and conformational analysis* Second ed.; Wiley-VCH: 2000.
65. Breeze, A. L., Isotope-filtered NMR methods for the study of biomolecular structure and interactions. *Prog. Nucl. Magn. Reson. Spectrosc.* **2000,** *36* (4), 323-372.
66. Rinaldi, P. L., Heteronuclear 2D-NOE spectroscopy. *J. Am. Chem. Soc* **1983,** *105* (15), 5167-5168.
67. Repasky, M. P.; Shelley, M.; Friesner, R. A., Flexible Ligand Docking with Glide. *Curr. Protoc. Bioinform.* **2007,** *18* (1), 8.12.1-8.12.36.
68. Naas, T.; Oueslati, S.; Bonnin, R. A.; Dabos, M. L.; Zavala, A.; Dortet, L.; Retailleau, P.; Iorga, B. I., Beta-lactamase database (BLDB) – structure and function. *J. Enzyme. Inhib. Med. Chem.* **2017,** *32* (1), 917-919.
69. Ballatore, C.; Huryn, D. M.; Smith III, A. B., Carboxylic Acid (Bio)Isosteres in Drug Design. *ChemMedChem.* **2013,** *8* (3), 385-395.
70. Kombo, D. C.; Tallapragada, K.; Jain, R.; Chewning, J.; Mazurov, A. A.; Speake, J. D.; Hauser, T. A.; Toler, S., 3D molecular descriptors important for clinical success. *J. Chem. Inf. Model.* **2013,** *53* (2), 327-42.
71. Kraut, J., Serine Proteases: Structure and Mechanism of Catalysis. *Annu. Rev. Biochem.* **1977,** *46* (1), 331-358.
72. Guo, Y.; Wang, J.; Niu, G.; Shui, W.; Sun, Y.; Zhou, H.; Zhang, Y.; Yang, C.; Lou, Z.; Rao, Z., A structural view of the antibiotic degradation enzyme NDM-1 from a superbug. *Protein & cell* **2011,** *2* (5), 384-94.
73. Gilpin, M. L., Payne, D.J., Bateson, J.H. Pyrrolidine and thiazole derivatives with metallo-b-lactamase inhibitory properties. 1997. 1997.
74. Melnikova, D. L.; Skirda, V. D.; Nesmelova, I. V., Effect of Reducing Agent TCEP on Translational Diffusion and Supramolecular Assembly in Aqueous Solutions of α-Casein. *J. Phys. Chem. B* **2019,** *123* (10), 2305-2315.
75. Harner, M. J.; Mueller, L.; Robbins, K. J.; Reily, M. D., NMR in drug design. *Arch. Biochem. Biophys.* **2017,** *628*, 132-147.
76. Schwalbe, H., Applied NMR Spectroscopy for Chemists and Life Scientists. By Oliver Zerbe and Simon Jurt. *Angew. Chem. Int. Ed.* **2014,** *53* (49), 13324-13324.
77. Oliver Zerbe, S. J., *Applied NMR Spectroscopy for Chemists and Life Scientists*. Wiley: 2014.
78. Palica, K.; Vorácová, M.; Skagseth, S.; Andersson Rasmussen, A.; Allander, L.; Hubert, M.; Sandegren, L.; Schrøder Leiros, H.-K.; Andersson, H.; Erdélyi, M., Metallo-β-Lactamase Inhibitor Phosphonamidate Monoesters. *ACS omega* **2022,** *7* (5), 4550-4562.
79. Rivière, G.; Oueslati, S.; Gayral, M.; Créchet, J.-B.; Nhiri, N.; Jacquet, E.; Cintrat, J.-C.; Giraud, F.; van Heijenoort, C.; Lescop, E.; Pethe, S.; Iorga, B. I.; Naas, T.; Guittet, E.; Morellet, N., NMR Characterization of the Influence of Zinc(II) Ions on the Structural and Dynamic Behavior of the New Delhi Metallo-β-Lactamase-1 and on the Binding with Flavonols as Inhibitors. *ACS omega* **2020,** *5* (18), 10466-10480.
80. Yao, C.; Wu, Q.; Xu, G.; Li, C., NMR backbone resonance assignment of New Delhi metallo-beta-lactamase. *Biomol. NMR. Assign.* **2017,** *11* (2), 239-242.

81. Wieske, L. H. E.; Bogaerts, J.; Leding, A. A. M.; Wilcox, S.; Andersson Rasmussen, A.; Leszczak, K.; Turunen, L.; Herrebout, W. A.; Hubert, M.; Bayer, A.; Erdélyi, M., NMR Backbone Assignment of VIM-2 and Identification of the Active Enantiomer of a Potential Inhibitor. *ACS Med. Chem. Lett.* **2022,** *13* (2), 257-261.
82. Busi, B.; Yarava, J. R.; Bertarello, A.; Freymond, F.; Adamski, W.; Maurin, D.; Hiller, M.; Oschkinat, H.; Blackledge, M.; Emsley, L., Similarities and Differences among Protein Dynamics Studied by Variable Temperature Nuclear Magnetic Resonance Relaxation. *J. Phys. Chem. B* **2021,** *125* (9), 2212-2221.
83. Wang, R.; Lai, T.-P.; Gao, P.; Zhang, H.; Ho, P.-L.; Woo, P. C.-Y.; Ma, G.; Kao, R. Y.-T.; Li, H.; Sun, H., Bismuth antimicrobial drugs serve as broad-spectrum metallo-β-lactamase inhibitors. *Nat. Commun.* **2018,** *9* (1), 439.
84. Brünger, A. T., X-ray crystallography and NMR reveal complementary views of structure and dynamics. *Nat. Struct. Biol.* **1997,** *4 Suppl*, 862-5.
85. Sun, Z.; Hu, L.; Sankaran, B.; Prasad, B. V. V.; Palzkill, T., Differential active site requirements for NDM-1 β-lactamase hydrolysis of carbapenem versus penicillin and cephalosporin antibiotics. *Nat. Commun.* **2018,** *9* (1), 4524.
86. van Groesen, E.; Lohans, C. T.; Brem, J.; Aertker, K. M. J.; Claridge, T. D. W.; Schofield, C. J., (19) F NMR Monitoring of Reversible Protein Post-Translational Modifications: Class D β-Lactamase Carbamylation and Inhibition. *Chemistry* **2019,** *25* (51), 11837-11841.
87. Pemberton, O. A.; Jaishankar, P.; Akhtar, A.; Adams, J. L.; Shaw, L. N.; Renslo, A. R.; Chen, Y., Heteroaryl Phosphonates as Noncovalent Inhibitors of Both Serine- and Metallocarbapenemases. *J. Med. Chem.* **2019,** *62* (18), 8480-8496.
88. Ma, G.; Wang, S.; Wu, K.; Zhang, W.; Ahmad, A.; Hao, Q.; Lei, X.; Zhang, H., Structure-guided optimization of D-captopril for discovery of potent NDM-1 inhibitors. *Bioorg. Med. Chem.* **2021,** *29*, 115902.
89. Etter, M. C., Hydrogen bonds as design elements in organic chemistry. *J. Phys. Chem. A* **1991,** *95* (12), 4601-4610.
90. Pietruś, W.; Kafel, R.; Bojarski, A. J.; Kurczab, R., Hydrogen Bonds with Fluorine in Ligand–Protein Complexes-the PDB Analysis and Energy Calculations. *Molecules* **2022,** *27* (3).

Acta Universitatis Upsaliensis

Digital Comprehensive Summaries of Uppsala Dissertations from the Faculty of Science and Technology 2170

Editor: The Dean of the Faculty of Science and Technology

A doctoral dissertation from the Faculty of Science and Technology, Uppsala University, is usually a summary of a number of papers. A few copies of the complete dissertation are kept at major Swedish research libraries, while the summary alone is distributed internationally through the series Digital Comprehensive Summaries of Uppsala Dissertations from the Faculty of Science and Technology. (Prior to January, 2005, the series was published under the title "Comprehensive Summaries of Uppsala Dissertations from the Faculty of Science and Technology".)

Distribution: publications.uu.se
urn:nbn:se:uu:diva-481327

ACTA
UNIVERSITATIS
UPSALIENSIS
UPPSALA
2022